Master's thesis

NTNU
Norwegian University of Science and Technology
Faculty of Natural Sciences
Department of Chemistry

Tina Maria Bruns

Quantifying Growth of Anisotropic Gold Nanoparticles and Understanding Growth Mechanisms

Master's thesis in Chemical Engineering and Biotechnology
Supervisor: Sulalit Bandyopadhyay and Trond Peder Flaten
Co-supervisor: Karthik Raghunathan and Katharina Zürbes
September 2021

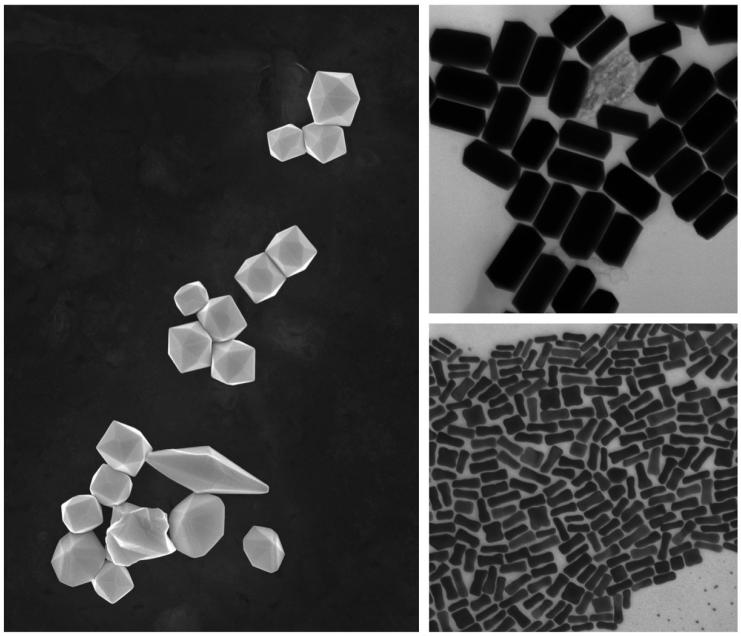

NTNU
Norwegian University of
Science and Technology

Tina Maria Bruns

Quantifying Growth of Anisotropic Gold Nanoparticles and Understanding Growth Mechanisms

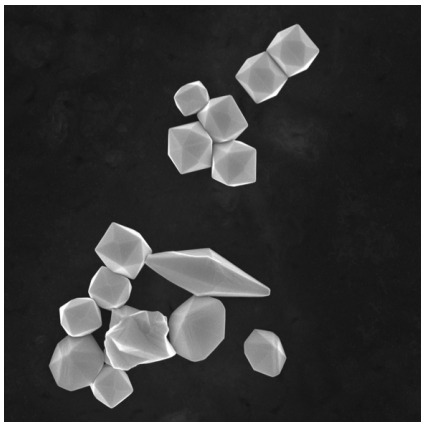

Master's thesis in Chemical Engineering and Biotechnology
Supervisor: Sulalit Bandyopadhyay and Trond Peder Flaten
Co-supervisor: Karthik Raghunathan and Katharina Zürbes
September 2021

Norwegian University of Science and Technology
Faculty of Natural Sciences
Department of Chemistry

NTNU
Norwegian University of
Science and Technology

Acknowledgements

First and foremost, I would like to thank my supervision team for making this master thesis a reality and guiding me through this till the end.

I am grateful to my supervisor Sulalit Bandyopadhyay for giving me the opportunity to do this project, for setting aside time for weekly meetings and for having an open door for me in his busy schedule.

I could not have done this without my amazing co-supervisors Karthik Raghunathan and Katharina Zürbes. I am eternally grateful for all the help, patience and support you have given me during this work. Thank you for caring about the project and giving me close follow-up by checking in, having meetings, popping by the laboratory and always being available for me.

Thank to my internal supervisor Trond Peder Flaten at IKJ for administering and taking care of the formal processes involved with the thesis and always replying quickly to my emails.

A great thanks to all the people working in the Ugelstad Laboratory for making the hours of lab work pass more quickly, and for helping me understand things along the way.

Finally, a huge thanks to all my flatmates, family and friends who have provided me with both moral and technical support. A special thanks to my grandfather, David Bruns, for spending time proofreading at the last minute.

Abstract

The study of anisotropic gold nanoparticles (AuNPs) and their growth is an area of great interest due to their remarkable biocompatible and plasmonic properties. These properties are highly size- and shape-dependent, making it necessary to understand the growth and to tune the method to gain control over the shapes and properties of the AuNPs.

This work focuses on the seed-mediated, silver-assisted growth and expanding the knowledge obtained by Raghunathan et al.[1] and the knowledge gained in my project leading up to this work.[2] An experimental approach to understand the growth was used, exploring the effects of the reducing agent, Oleic Acid (OA), pH and ions as the main topics.

The effects of varying amounts of OA were explored with an alternative reducing agent, Tannic Acid (TA), in a screening design consisting of 13 experiments. The pH and amount of $AgNO_3$ were also varied. Mathematical models were made based on the fit from the resulting lengths and aspect ratios, and it was found that the syntheses rarely yielded AuNPs at pH 1.5.

A higher pH (11) and a higher amount of OA (200 µL) were studied. Further, to decouple the effects of pH, the effect of the ions added to change the pH were investigated by adding the same amount of ions at different times in the synthesis. This was done with 0, 20 and 200 µL OA. It was seen that the amount of OA had a dominating effect on the system, while the time of adding ions had little to no effect on the final product. Characterization of the final AuNPs was mainly done by UV-Vis and S(T)EM.

A yield study was conducted using microwave plasma atomic emission spectrometry for some of the syntheses variations. The yield was found to be 12.2, 25.3 and 94.9 % for syntheses without silver, with silver and with silver and 20 µL OA, respectively. This pointed towards the dual role of OA as co-surfactant and reducing agent.

Finally, the work was rounded off by a discussion around possible growth mechanisms.

Table of Contents

List of Figures

List of Tables

1 Introduction

Gold is a well-known element and will likely bring to mind a valuable shiny golden metal. Gold on the nanoscale however, has a very different appearance. Gold nanoparticles (AuNPs) may have a range of different colours like pink, red or even blue. The colours of these nanoparticles (NPs) depend on *size* and *shape*, which, more importantly, result in different properties.[3] These shapes and sizes are tunable. The challenge lies in understanding the *hows* and *whys*.

AuNPs have been a topic of great interest for many years, especially in the past two decades, where anisotropic (non-spherical) AuNPs have been widely studied to better understand their growth and properties.[4] Some of the reason behind this great fascination for AuNPs is their remarkable plasmonic and biomedical properties. They have been found to have a low cytotoxicity and good affinity to biological material, making them suitable for biomedical applications like imaging, sensing and photothermal therapy.[5] [6]

1.1 Plasmonic properties

One of the most striking features of AuNPs is their plasmonic properties.[4] When an electromagnetic wave interacts with conductive NPs smaller than the incident wavelength, the optical phenomenon Localized Surface Plasmon Resonance (LSPR) occurs. The resonance occurs when the incident frequency matches the oscillation frequency, which will cause the collective excitement of electrons.[7] [3] Figure 1 illustrates the resulting electric field caused by the oscillation of particles with the excited electrons shown as an electron cloud.

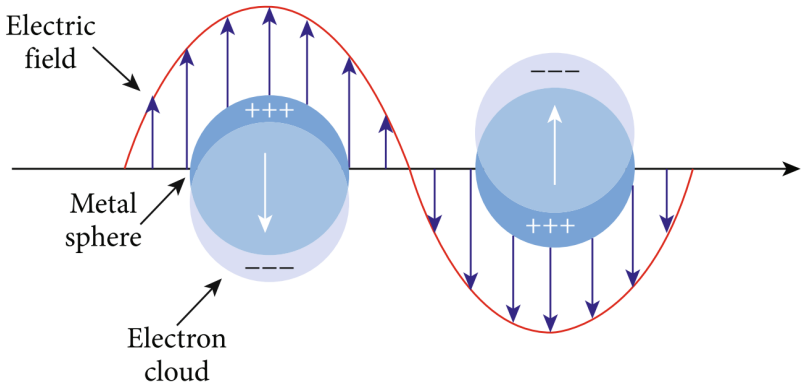

Figure 1: Localized Surface Plasmon Resonance of nanoparticles.[8]

The LSPR strongly depends on the composition, size, shape, dielectric environment and distance between the NPs.[7] Different shapes of AuNPs will cause varying absorbance spectra, making this a helpful tool when characterizing shapes in a solution.[9] [3] Anisotropic NPs are especially interesting as they display multiple plasmon bands. For example, gold nanorods (AuNRs) has one band for the longitudinal (long) axis, and one for the transverse (short) axis of the rods.[4] Figure 2a shows a typical absorbance spectrum obtained for AuNRs.

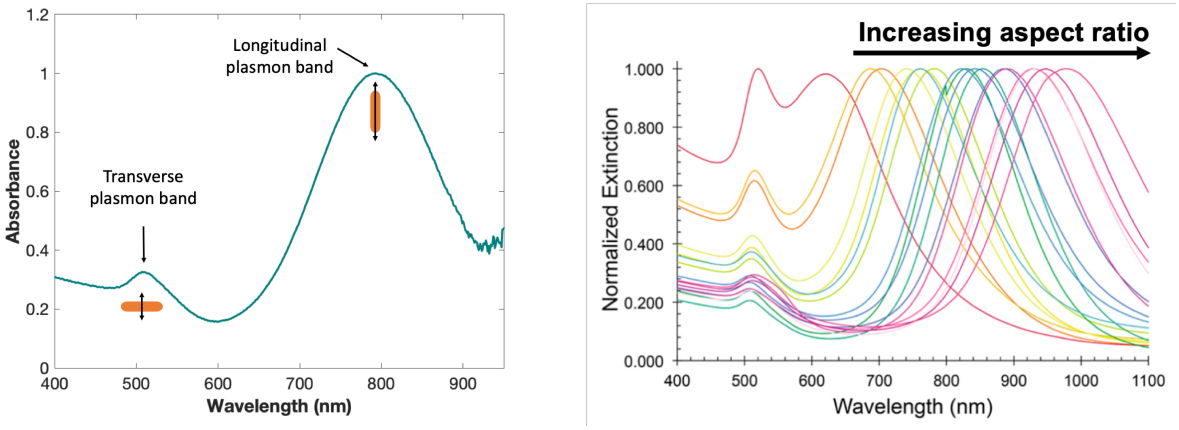

(a) (b)

Figure 2: a) Gold nanorods give two plasmon bands, transverse and longitudinal.[2] b) Increased aspect ratio of these rods gives higher wavelengths for the longitudinal LSPR bands.[10]

The energy of the AuNR longitudinal plasmon band is strongly influenced by the ratio between the long and short axes. The aspect ratio (AR) of the AuNRs is expressed by equation 1:

$$\mathrm{AR} = \frac{L}{D} \tag{1}$$

L and D correspond to the length (long axis) and diameter (short axis) of the AuNR respectively.[5] Increased aspect ratio of AuNRs shifts the longitudinal LSPR bands to higher wavelengths (red-shift), as indicated by the black arrow in Figure 2b.[4] [11]

1.2 Synthesis of Gold Nanoparticles

Throughout the years, several ways of synthesizing AuNPs have been used, and the methods have been modified as the parameters have become better understood.[4] As the properties of NPs are highly size and shape dependent, obtaining a high yield and uniformity is desired. The two main synthesis categories are the top-down and the bottom-up approaches.

In top-down approach, AuNPs are obtained through a combination of different physical lithography processes and gold deposition, while in the bottom-up approach, AuNPs are synthesized through nucleation in aqueous solutions followed by growth, where gold salts are usually used to provide the gold source through reduction.[3]

The seed-mediated, surface-directed (silver-assisted) synthesis method is a widely used bottom-up approach to obtain AuNPs.[5]. In this method, AuNPs are formed by adding small Au seeds to an aqueous "growth solution" consisting of surfactant (usually CTAB),

ionic gold (usually Au(III)Cl_4^-), a weak reducing agent and ionic silver.[12] Figure 3 illustrates this with ascorbic acid (AA) as the weak reducing agent. Equation 2 shows the reduction of Au^{3+} to elementary gold nanoparticles by using a weak reducing agent and seed.

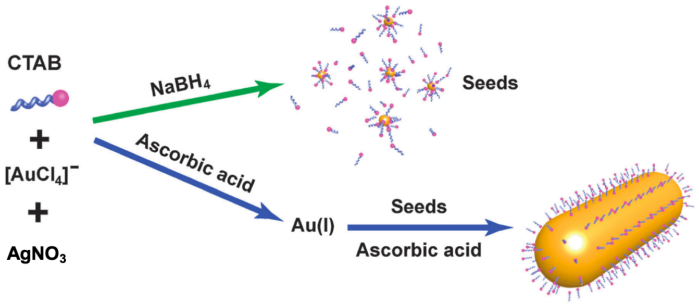

Figure 3: Schematic illustration of the seed-mediated growth method of gold nanorods.[3]

$$Au^{3+} \xrightarrow{\text{Weak reducing agent}} Au^{+} \xrightarrow{Au^0\ (\text{seed})} Au^0\ (\text{nanoparticles}) \tag{2}$$

To further understand *how* the synthesis results in these AuNRs, it is necessary to know more about nucleation and growth. Some proposed mechanisms will also be described later.

1.3 Nucleation and Growth

The LaMer model, illustrated in Figure 4, describes the general mechanism of the NP formation process through nucleation and growth. Nucleation, in short, is a thermodynamic model describing the appearance of a new phase - the nucleus - in the metastable primary phase.[13] The classical nucleation theory describes the theory behind this phenomenon through applying the fact that a thermodynamic system tends to minimize its Gibbs free energy. There are two types of nucleation: homogeneous and heterogeneous. Homogeneous nucleation is spontaneous but requires a supercritical state such as supersaturation. Heterogeneous nucleation occurs at nucleation sites on solid surfaces.

In the LaMer diagram, the red curve represents the theoretical monomer concentration in the solution as a function of time. At first, the concentration of monomers is increased (usually due to reduction in case of metallic NPs). At t_1 the critical supersaturation level (C_S) is reached and homogeneous nucleation is possible, but effectively infinite. At t_2 the saturation reaches a level (C_C) at which the energy barrier for nucleation can be overcome, leading to a rapid self-nucleation. This rapid nucleation causes the supersaturation level to lower to below C_C (at t_3), ending the nucleation period. Then, growth occurs by diffusion of further monomers in solution to the particle surfaces. This growth can be interpreted as heterogeneous nucleation/growth.[15]

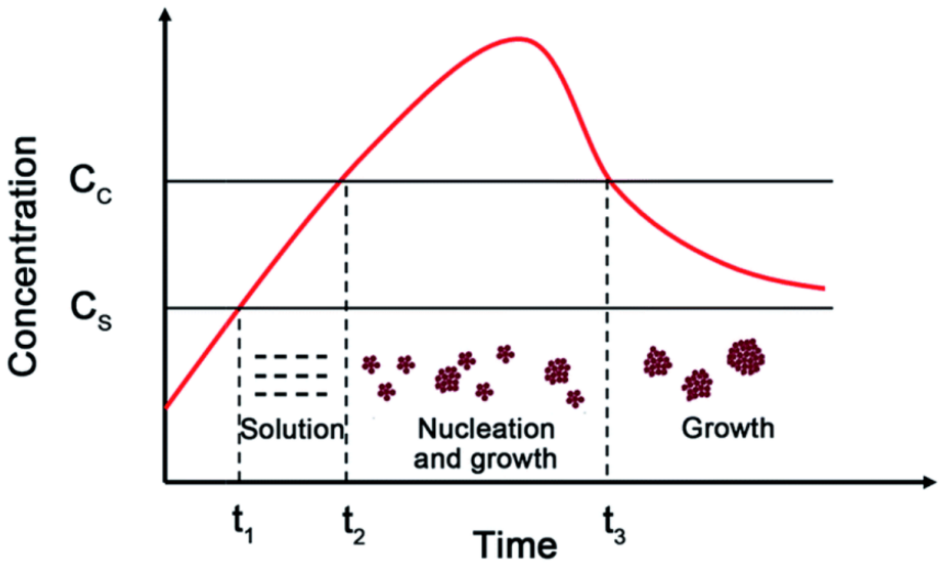

Figure 4: LaMer diagram describing general nucleation and growth.[14]

In the AuNP synthesis, the growth of the "seeds" follow the process of homogeneous nucleation. These seeds are furthermore used as the solid surface providing nucleation sites for the heterogeneous nucleation.

1.4 Growth mechanism and kinetics

As mentioned in section 1.3, the NPs start growing at some point. However, how the growth occurs can be unclear, and many have tried to explain this for anisotropic AuNPs. The properties of AuNPs are highly shape dependent, making control of the parameters critical for their functionalization.[16] AuNRs are of particular interest, and a lot of effort has been put into understanding these specifically. So far, it is well established that the growth is dependent on several variables in the synthesis. Systematic experiments have been carried out to show how individual factors like temperature, pH, reagents and their concentration all affect the final product. Not only does changing the individual variables have an effect, but the interplay between them must also be considered.[10] Ultimately, a deeper understanding and control of the growth mechanism is required to optimize the synthesis and gain control to obtain the desired NPs.[4]

Some theories explaining the growth of AuNRs have been suggested. A closer look at some of the proposed mechanisms may give a better understanding of how the growth is happening. Mechanisms as reviewed by Lohse et al.[4] are the following:

1) Silver underpotential deposition
2) Surfactant templating
3) Face-specific capping

These are further illustrated and described in Figure 5:

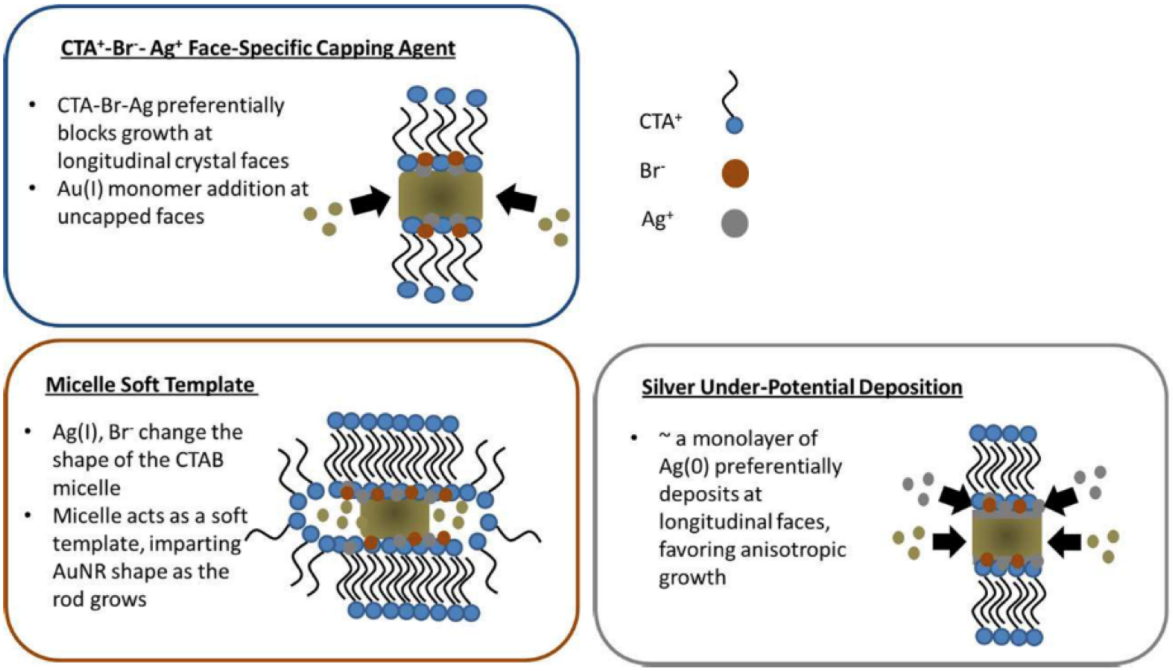

Figure 5: Three mechanisms of AuNPs growth.[4]

Face-specific capping is based on the theory that CTAB-Ag preferentially binds to certain faces, blocking the growth of Au here and leading to symmetry breaking.[17] Silver Under-Potential Deposition (UPD) is similar in that it suggested that one of the sides is preferred but it differs in that it proposes that Ag^+ ions are reduced before Au, and deposit on the longitudinal faces ({110}) due to UPD. This leads to surface passivation and slows the growth so that Au deposits on the more energetically favorable faces, leading to anisotropic growth.[18] The Micelle Soft Template theory suggests that Ag^+ and Br^- alter the shape of the CTAB micelles in to a cylindrical shaped micelle, which provides a space in which the AuNRs can grow.

A zipping mechanism was suggested, where the formation of the CTAB bilayer on the nanorod surface may assist nanorod formation as more Au is introduced.[19] Figure 6 illustrates this.

It has also been suggested that AuNRs don't grow uniformly and steadily. Rather, they grow according to a "popcorn"-like mechanism in which individual seeds are inactive for some time before they suddenly and rapidly grow into rods at different times.[12]

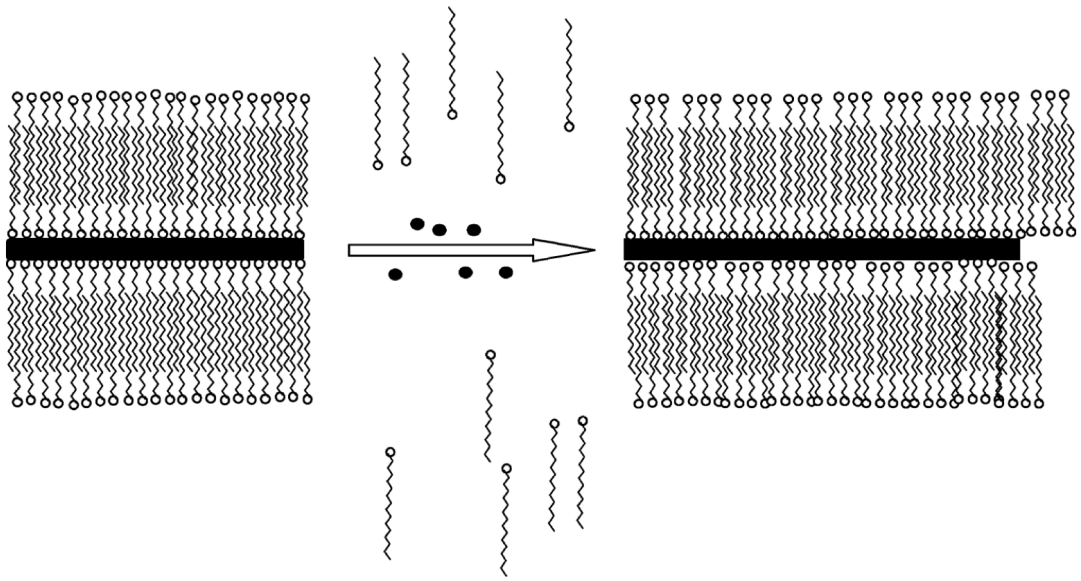

Figure 6: Zipping mechanism.[19] CTAB (squiggles) forming a bilayer on the gold (black) surface.

Khlebtsov et al.[20] described how overgrowth could occur on nanorods according to the surfactant and co-surfactant used in the synthesis. Their results implied that the less stable {110} facets are unlikely to be coated with Au owing to the stronger interaction with the surfactant molecules. Figure 7 illustrates fast overgrowth as a result of high amount of AA in the common 0.1 M CTAB growth solution and slow overgrowth by using a binary surfactant mixture of CTAB and NaOL.

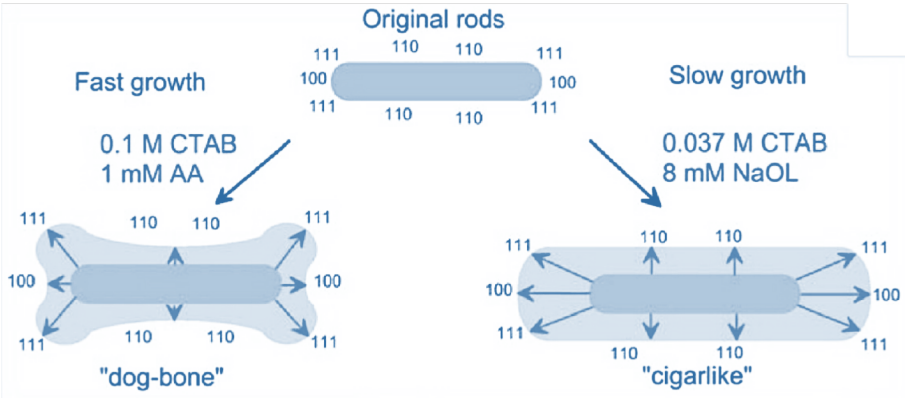

Figure 7: Illustration of fast and slow overgrowth of AuNRs.[20]

The growth can be further understood by having a closer look at the effect of some of the individual parameters involved. These will be further explained in the next section.

1.5 Effects of various parameters

In the growth of the AuNPs, the parameters in the synthesis have various effects on the system.

1.5.1 Surfactant

Dissolved surfactants in solution can form micelles above certain concentration, providing an environment for the NPs to grow. Ions in the solution have an affect on the size of the micelles. CTAB is commonly used for AuNRs and forms a bilayer around the AuNP in solution.[21] The effect of the counterion in the surfactant has been closely studied to observe the effect of this and find out if other counterions/surfactants can be used.[22] Chloride has been suggested as an alternative halide to CTA+ instead of bromide. However, the lower affinity of Cl ions for Au surfaces compared to Br could possibly result in a denser micellar layer.[23]

1.5.2 Co-surfactant

Co-surfactants are sometimes introduced to the system to create a binary surfactant mixture, possibly leading to mixed micelles.[24] The structures of two co-surfactants are given in Figure 8 alongside CTAB. Oleic Acid (OA) and Sodium Oleate (NaOL) are similar in structure and have similar lengths ($\sim$ 2 nm) as CTAB.[25] [26]

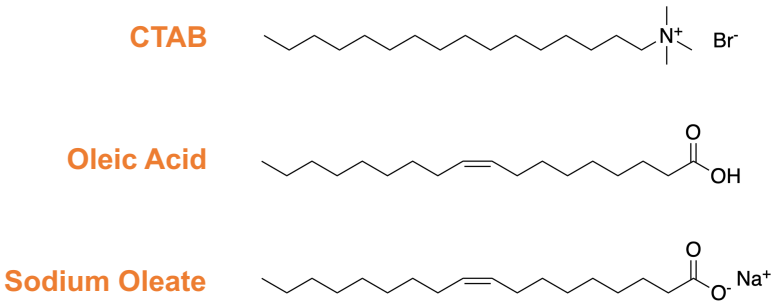

Figure 8: Structures of hexadecyltrimethylammonium bromide (CTAB), oleic acid and sodium oleate.

Raghunathan et al.[1] conducted a study where the growth of AuNPs by the seed-mediated growth was explored. Amongst other factors, they looked into the effect of the co-surfactant OA and varying the pH before adding AA. When the pH was unchanged, 20 µL OA gave "etched rods" similar to what is described as "dog-bone" in Figure 7.

Ye et al.[25] reported the effects of using a binary surfactant mixture of CTAB and NaOL. They showed that by lowering the amount of CTAB and varying the amount of NaOL, they could tune the length and AR of the AuNRs. As the dimensions of AuNRs became larger, they started to develop clear faceting, as shown in Figure 9.

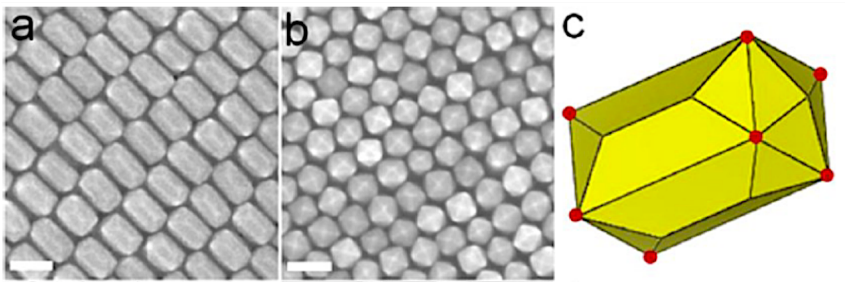

Figure 9: Elongated tetrahexahedra.[25]

In the same work[25] it was suggested that the concentration of CTAB in the standard method (0.1 M) would not allow for the same level of control over the AuNR's size uniformity and tunability as for what they used (0.037 M CTAB).

In a work by Bandyopadhyay et al.[27] they showed how shapes could be tuned by binary surfactant mixtures. CTAB was used in combination with DDAB and DDAI, and a schematic with some of the resulting shapes are shown in Figure 10

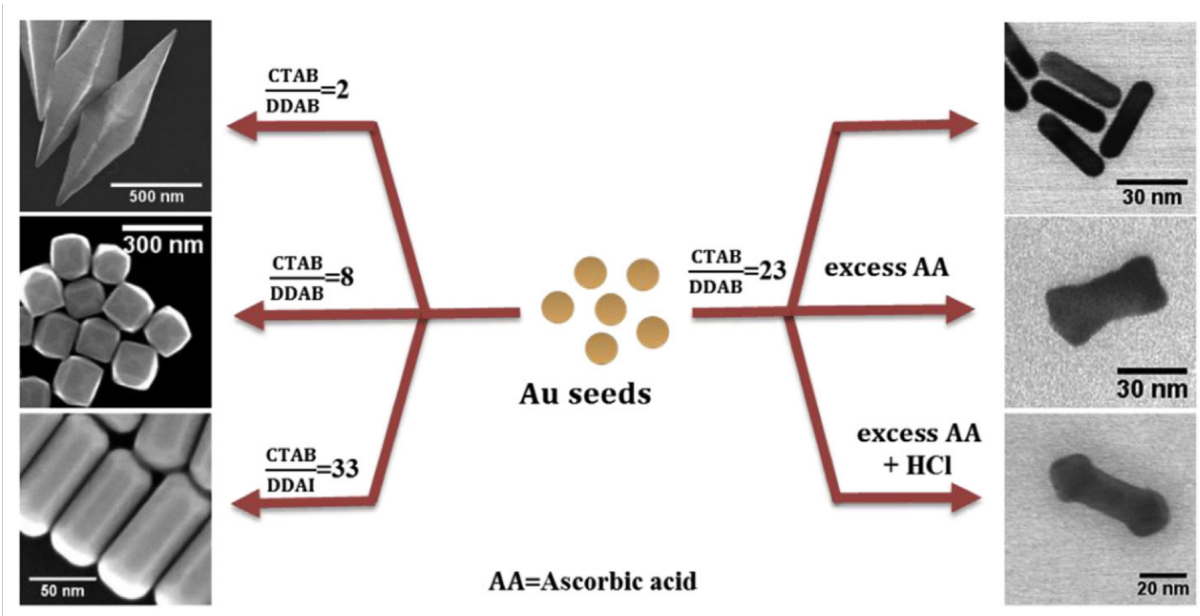

Figure 10: Schematic showing various shapes resulting from varying binary surfactant mixtures.[27]

1.5.3 Silver Nitrate

As briefly mentioned in section 1.4, silver has an effect on the shape-control of the AuNPs. This could typically be used to promote anisotropic rather than isotropic particles.[16] Tong et al.[16] described how $AgNO_3$ plays a part in the symmetry-breaking and the concentration affects the AR. Figure 11 briefly shows this.

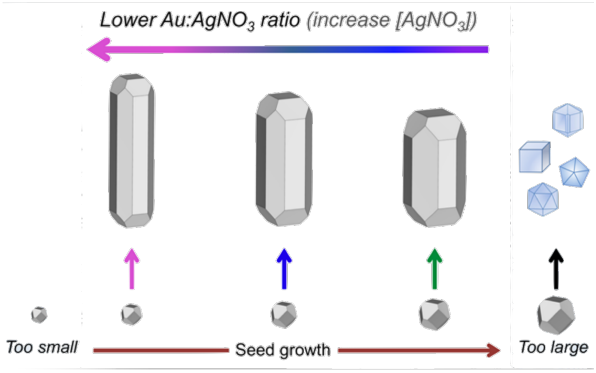

Figure 11: Effect of Silver Nitrate concentration on AuNRs width and aspect ratio. [16]

By increasing the silver nitrate concentration, higher AR can be achieved. [28] However, at a certain concentration, further increasing $AgNO_3$ will no longer increase the AR. [16]

1.5.4 Reducing Agent

Ascorbic acid (AA) is used as a reducing agent in the general synthesis of AuNPs. Gold ions are introduced to the system in the form of $HAuCl_4$. The gold ions are Au^{3+}, and are reduced to Au^{1+} by AA.

The pH of a solution could have an effect on the reduction potential of the reducing agent, which is especially relevant for AA as it has two pK_a-values of 4.04 and 11.7 (at 25°C). [29] Figure 12 gives a schematic with the structure of AA and the reduction at both pK_a-values.

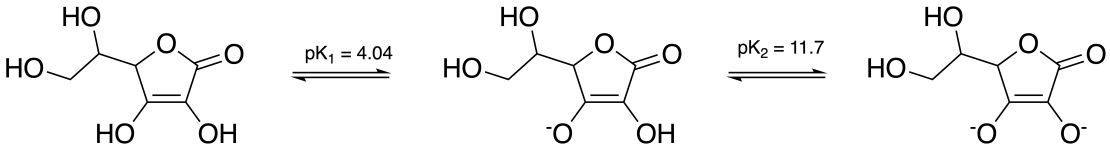

Figure 12: Ascorbic acid's two pK_a-values

In the study by Raghunathan et al. [1] they showed that a high amount of AA (400 µL) led to etched rods instead of AuNRs as obtained with less AA (135 µL).

Sometimes a single parameter can have multiple roles. Though mainly added as a co-surfactant, OA can also act like a reducing agent. [1]

Although AA is the most commonly used reducing agent in the seed-mediated synthesis, Tannic Acid (TA) could also be one to explore as it has been used as a reducing agent for other types of AuNP syntheses. [30] [31] [32] Figure 13 displays the structure of TA which is a very large molecule compared to AA.

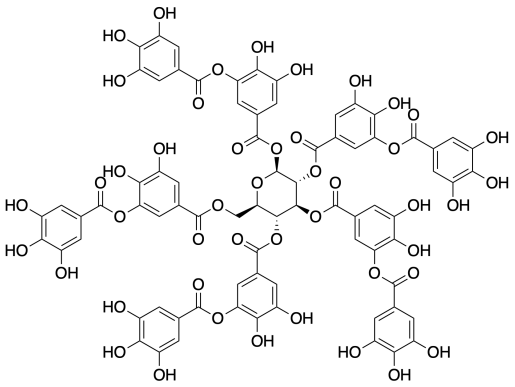

Figure 13: Structure of Tannic Acid

The use of TA in the seed-mediated growth method resulted in "nanoearbuds" in a work by Roy et al.[30] They used a binary surfactant mixture of CTAC and BDAC, and suggested the mechanism as shown in Figure 14.

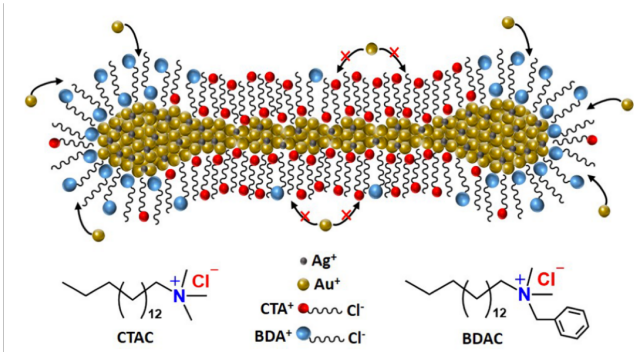

Figure 14: Nanoearbud formation in the presence of binary surfactants.[30]

It was suggested that there would be a higher amount of CTAC monomers on the lateral facets with a tighter packing due to the smaller headgroup. This would allow less growth in this direction. The BDAC with its larger headgroup would deposit on the ends, much less tightly, allowing for Au to deposit here.[30]

1.5.5 Effect of pH

The effect of pH is known to have an effect on the system in some way.[25] [27] [33]

In the work by Raghunathan et al.[1] the effect of changing the pH before adding AA was explored. pH seemed to have a dominating role in controlling the growth of the AuNPs, and some of the resulting NPs are summarized in Figure 15.

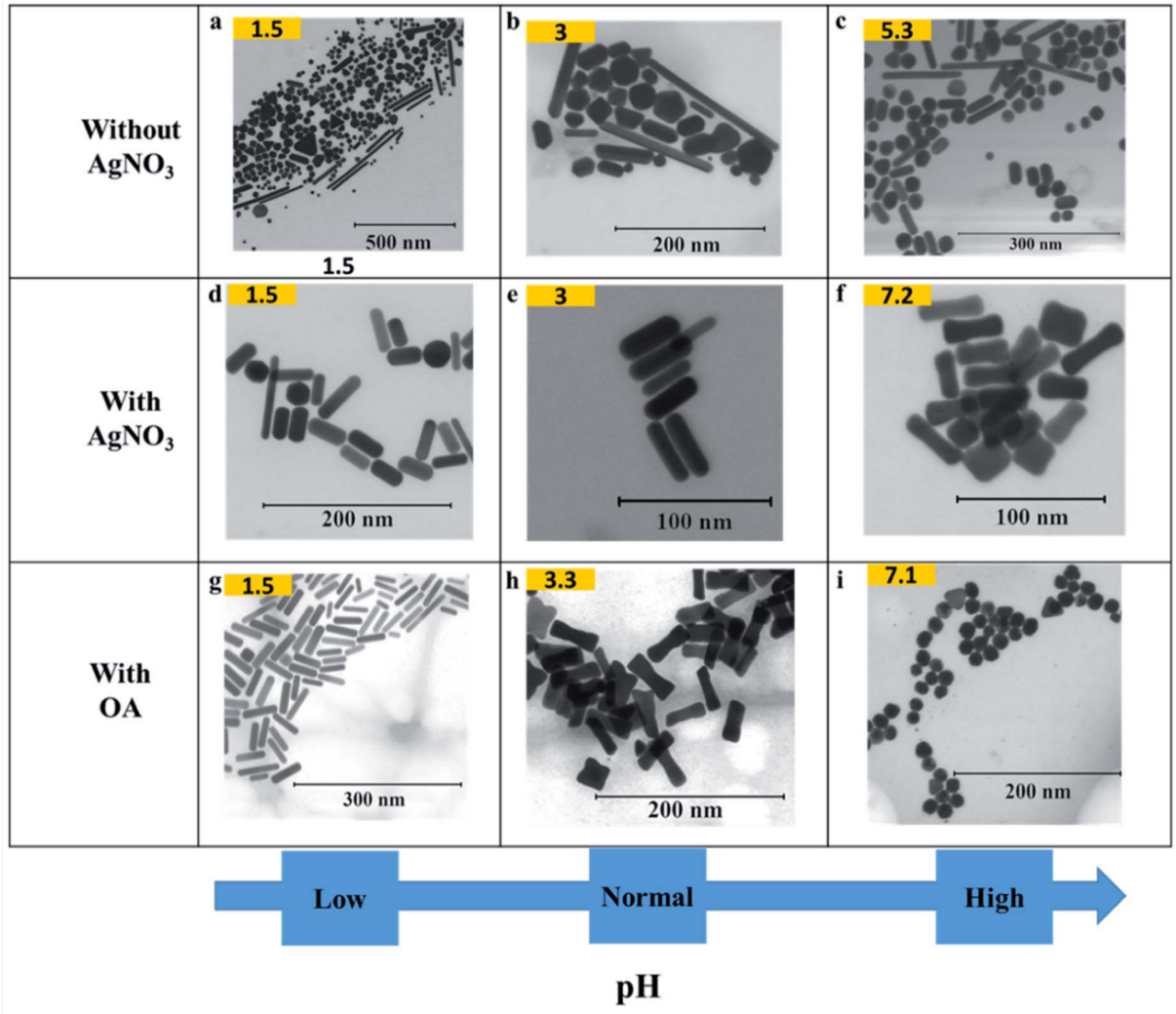

Figure 15: S(T)EM images showing the effect of pH on the shape of AuNPs.[1]

As mentioned in section 1.5.4, the reduction potential of the reducing agent may be affected by the pH. This is expected to excert an influence on the morphologies obtained.[1]

Wu et al.[33] increased the pH to 11.5 using NaOH which first resulted in branched nanocrystals. Later (after 52 h storage at room temperature) these had transformed into spheres. Figure 16 show the resulting shapes.

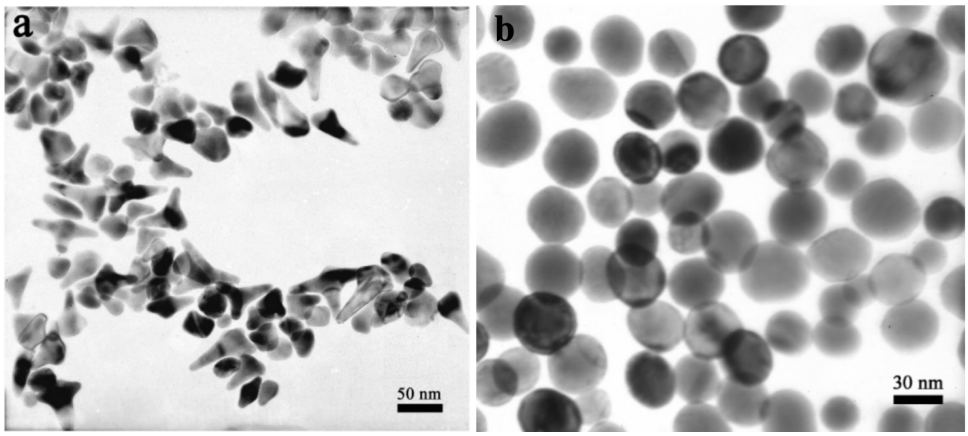

Figure 16: Branched nanocrystals and spherical nanoparticles obtained at high pH.[33]

1.6 Preliminary work

Following is a short summary of the main points from the project leading up to this work. Here, the effects of varying the pH in the beginning of the seed-mediated silver-assisted growth synthesis of AuNPs were studied.[2] Starting-pH values of 1.5, 3, ∼6 (MQ-water) and 10 were explored. Some experiments were also done without silver, and some with a binary surfactant mixture using 20 µL OA.

By measuring the pH at every step of the synthesis, it was found that the pH of the solution approached and stabilized at ∼3 when the gold ions were introduced to the system and did not change significantly beyond this step in the synthesis. It was suggested that the ions could have affected the micelle sizes, which could have an impact on the final AuNPs when considering surfactant templating (see section 1.4).

Through TEM-images and measurements it was seen that the pH did not have much effect on the shapes within each synthesis variation. The most significant difference was for 20 µL OA at pH 1.5, as it gave rods instead of etched rods (which were obtained at higher pH). The lengths and ARs did not show trends for the syntheses without OA, but decreased with increasing pH for 20 µL OA.

This was a small study, and further experiments were needed to explore the growth mechanism further.

1.7 Yield

When papers report "high yield" they are often referring to shape-yield. So if only rods were observed in S(T)EM and no other shapes; this would be considered a 100 % yield.[34] [35] Orendorff et al.[18] performed a detailed ICP-MS analysis and reported that only 15 % of the ions were converted into AuNPs by classical seed-mediated growth synthesis. Considering that the ever-increasing price of gold presents a significant challenge to real-world applications of AuNRs[36], it is essential to maximize the Au ions conversion.

2 Materials and Methods

The materials and methods used were similar to those in the preliminary work[2], with some modifications in the synthesis procedure.

2.1 Chemicals

All chemicals used in the synthesis of the AuNPs, as well as purities and providers are listed below, in Table 1.

Table 1: Chemicals used for synthesis of gold nanoparticles.

Chemical	Abbr.	Purity (%)	Provider
Hexadecyltrimethylammonium bromide	CTAB	99+	Acros Organics
Oleic Acid	OA	90	Sigma Aldrich
Gold(III) chloride trihydrate	$HAuCl_4$	-	Sigma Aldrich
Sodium borohydride	$NaBH_4$	99.3	Sigma Aldrich
Silver nitrate	$AgNO_3$	99.8	Sigma Aldrich
D-(-)-Isoascorbic acid	AA	99.3	Sigma Aldrich
Tannic Acid	TA		
Hydrochloric Acid	HCl	37	Sigma Aldrich
Sodium Hydroxide	NaOH	98.5 - 100.5	VWR

Distilled deionized water purified by a Millipore water purification system (MQ water) (pH $\sim$ 5.5 - 6.5) was used for the synthesis. HCl and NaOH were used to adjust the pH.

2.2 Synthesis of AuNPs

The silver-assisted, seed-mediated growth method was used for the syntheses in this work.[37] Variations to the general method were done by varying the amounts of certain parameters. The synthesis of the seed remained unchanged for all variations.

2.2.1 Au seed synthesis

First, 364.5 mg CTAB was dissolved in 5 mL water by heating it during constant stirring. The solution was cooled down to 25°C before 5 mL of 0.5 mM $HAuCl_4$ was added under rapid stirring. Then, a fresh solution of 4 mM $NaBH_4$ was prepared by quickly dissolving 3.9 mg $NaBH_4$ in 10 mL ice cold water, and then transferring 600 µL of this solution to 1 mL ice cold water. This 1.6 mL $NaBH_4$ was quickly added to the CTAB solution and stirred for 2-3 minutes before the stirring was stopped. Finally, the solution was set aside to grow for 30 minutes at room temperature.

2.2.2 Anisotropic AuNPs synthesis

1.2 g CTAB was dissolved in 15 mL water by heating the mixture to 75°C while stirring. When the CTAB had dissolved, it was cooled down to 35°C. 750 µL freshly prepared $AgNO_3$ (4 mM) was quickly added to the solution and stirred for 15 minutes. Then, 15 mL of $HAuCl_4$ (1 mM) was added and the solution was stirred for another 15 minutes. The stirring speed was increased to 1000 rpm before adding 135 µL of AA (128 mM). A colour change from yellow to clear was observed before finally 96 µL of the seed solution (described in 2.2.1) was added and the stirring was stopped. The solutions were kept at 35°C for overnight growth (minimum 12 h). Figure 17 shows a schematic of the steps involved. Steps in parentheses were optional and varied according to the variations explained later in section 2.2.3.

Washing was done two times to remove the excess surfactant from the solution. Each washing cycle was done by centrifuging the solution at 11000 rpm for 45 minutes, removing the supernatant and re-suspending the precipitated particles with water. After the final washing, the particles were re-suspended in 5 mL of water. The centrifuge used was from Eppendorf, model number 5810.

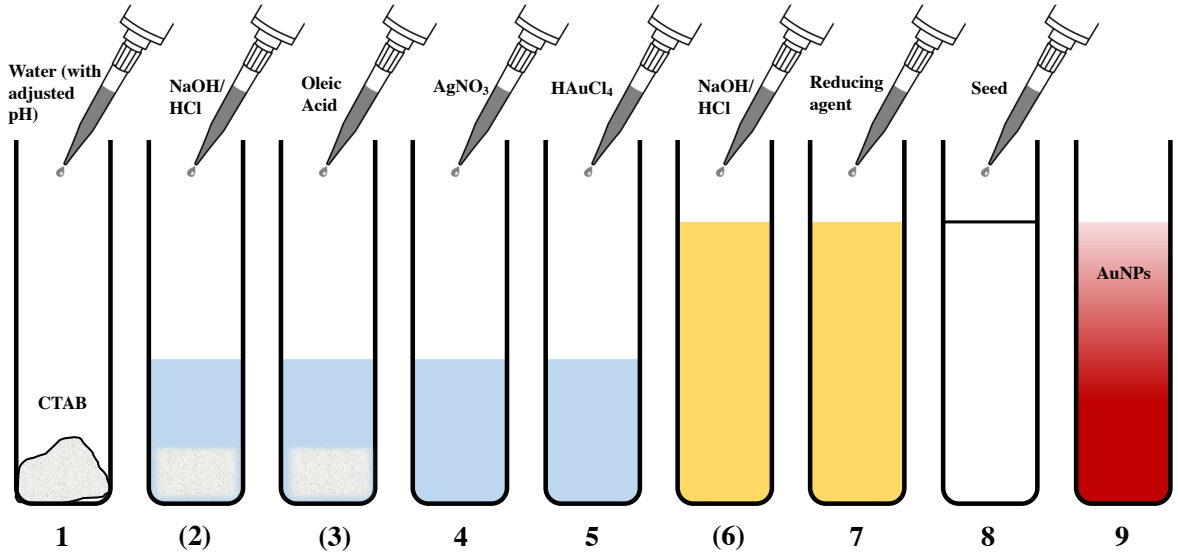

Figure 17: Schematic representation of seed- mediated synthesis of gold nanoparticles and all possible steps. Optional steps are in parentheses.

2.2.3 Variations in synthesis method

Variations to the general synthesis (explained in section 2.2.2) were done for most experiments, and are explained in this section. Refer to Figure 17 for steps. A summary of all the synthesis variations is listed in Table 2. A more detailed table listing each individual experiment can be found in section A.2.

Oleic Acid: Oleic acid (OA) was used to obtain a binary surfactant mixture. Varying amounts of OA were added as a co-surfactant to the CTAB solution at the beginning

of the synthesis (step 3). In this case, the surfactant mixture was heated to 95°C and removed from the heat when dissolved.

$AgNO_3$: The amount of $AgNO_3$ has been varied, and in some cases the reaction was done without any silver, skipping the step of adding $AgNO_3$ (step 4).

pH: The pH was varied using NaOH and HCl either at the start of the reaction, or in the growth solution directly before adding the AA (step 6). In the syntheses *starting* at different pH-values the pH of the MQ water was adjusted to pH-values from 1.5 to 11 before adding it to the CTAB (step 1).

Ions: The amount and concentration of ions is closely related to the pH. When studying the effect of ions, an exact amount of HCl or NaOH was added to the solution, instead of altering the pH to a set value. This was done either at the start of the reaction (step 2), or before adding AA (step 6).

Tannic Acid: TA (0.1 M) replaced AA as the reducing agent in some experiments. In this case, after adding the reducing agent, the solution was coloured by the TA and therefore a colour change to blank was not expected. Instead, a wait time of 1 minute was used before adding seed.

Table 2: Synthesis variations summary

Category	**pH/ions at start**	**OA (μL)**	**$AgNO_3$ (μL)**	**pH/ions before AA, TA**	**Reducing agent, amount (μL)**
Tannic Acid	unchanged	0 - 100	150 - 1500	pH 1.5 - 11	TA, 100-1650
Variation of pH and OA	pH 11	0, 20	0, 750	unchanged	AA, 135
	unchanged	0, 20	0, 750	pH 11	AA, 135
	pH 1.5, 3, 10, unchanged	200	750	unchanged	AA, 135
Fixed amount of ions at different steps	100 μL HCl/ 50 μL HCl/ 50 μL NaOH/ 100 μL NaOH	0, 20, 200	750	unchanged	AA, 135
	unchanged	0, 20, 200	750	100 μL HCl/ 50 μL HCl/ 50 μL NaOH/ 100 μL NaOH	AA, 135

2.3 Characterization

2.3.1 UV-Vis Spectroscopy

UV-Vis is a characterization technique where an incident light is passed through a solution to measure the intensity of the light transmitted through the sample. The technique is based on the Beer-Lambert law, expressed by equation 3, which shows that the absorbance, A, is directly proportional to the molar concentration, c.

$$A = -\log_{10}\left(\frac{I}{I_0}\right) = \varepsilon c l \tag{3}$$

Here, I and I_0 are the intensities of the transmitted and incident light respectively, ε is the molar absorption coefficient and l is the optical path length of the sample. [38]

This technique was used to measure the absorbance and find the LSPR of the AuNPs. As mentioned in section 1.1, solutions with AuNPs will absorb light at characteristic wavelengths, depending on the shapes and sizes of the NPs in the solution.

The UV-Vis spectra for the experiments in this study were measured with a Shimadzu UV-2401 PC spectrophotometer. Standard cuvettes with dimensions 12.5 x 12.5 x 45 mm were used.

2.3.2 Kinetics

The growth of the AuNPs was tracked by continuous UV-Vis measurements. After addition of seed, 3.5 mL of the solution was transferred into a cuvette and placed in the UV-Vis spectrophotometer. A temperature control for the UV-Vis was set at 35°C to maintain the temperature. The measurements were set to repeat 100 times, to continuously measure the absorbance spectrum from wavelength 1000 - 400 nm as the AuNPs grew. Every measurement took approximately 70 s, and the absorbance increased with time. The measurements were stopped when the absorbance spectrum did not increase any longer. If the particles were still growing at the end of the 100 runs, a new set of 100 runs was started until the growth stabilized and the absorbance spectra no longer increased with time.

Furthermore, the above-mentioned technique previously developed at the Ugelstad laboratory [1] was used to obtain the growth rate. The area under the curve was calculated for each individual absorbance spectrum, and the normalized area was plotted against time. A 4-parameter sigmoidal curve fit was used for the data, as given by equation 4.

$$y = y_0 + \frac{a}{1 + e^{\frac{-(x-x_0)}{b}}} \tag{4}$$

First order kinetics were assumed [1], and the parameters obtained from the sigmoidal fit (y_0, a, x_0, b) were used to find the growth rate, k.

Figure 18 gives an illustration of the procedure starting with the timed experiments from the spectrophotometer.

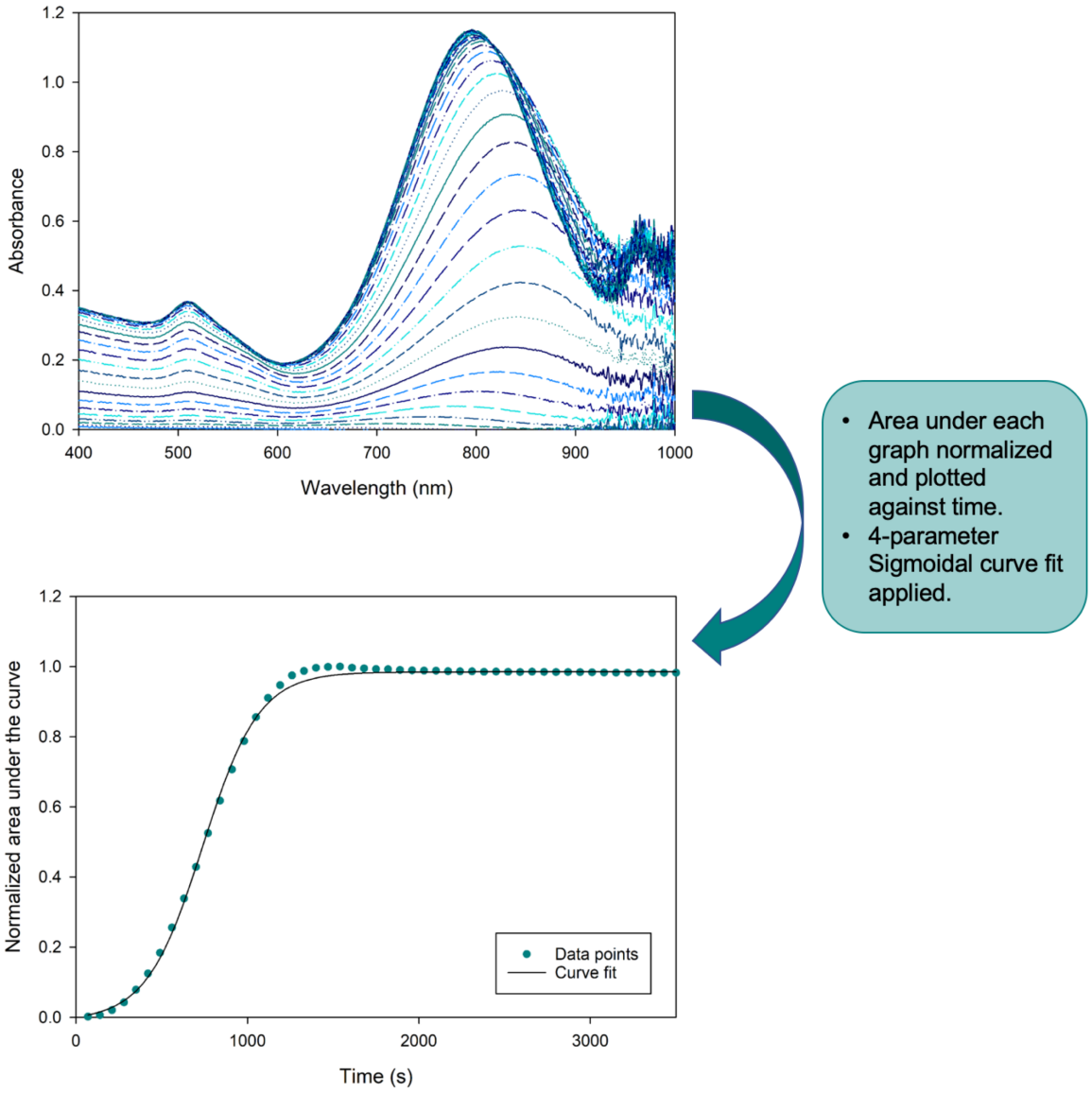

Figure 18: Schematic representation of modelling the data of the growth kinetics. Schematic based on method described by Raghunathan et al.[1]

2.3.3 S(T)EM

Scanning (transmission) electron microscopy (S(T)EM) is a method which combines the functionalities of scanning electron microscopy (SEM) and transmission electron microscopy (TEM)[39]. A focused beam of electrons is directed at a thin sample, and these electrons are scattered or transmitted according to interactions with the sample. The electrons are then captured by detectors and a virtual image is generated based on this. Figure 19 illustrates the difference in images when S(T)EM is used in SEM or TEM mode.

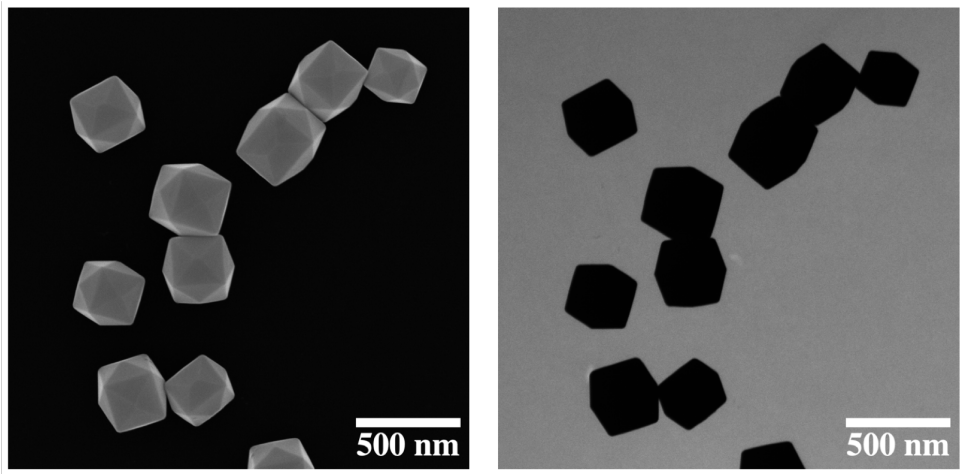

Figure 19: Images taken in SEM and TEM mode, respectively.

The images were acquired by secondary electron (SE) and bright field (BF) modes on a Hitachi SU9000 S(T)EM instrument. SE utilizes the scattered electrons and gives surface and bulk information (SEM mode). In BF mode only the unscattered electrons passing through the sample are detected (TEM mode), leading to a high-resolution image.

Image processing

ImageJ software was used to measure the NPs from the S(T)EM images. The software allows for quick analysis of spherical particles as it can calculate the area of these, but requires manual measurements of individual NPs in case of anisotropy.

2.3.4 MP-AES

Microwave Plasma Atomic Emission Spectroscopy (MP-AES) is a technique used to determine the concentration of specific ions in a solution. The method can have detection limits down to sub ppb levels.[40] For Au, the detection limit is reported to be 1.8 ppb.[41]

Quantification is done by introducing a liquid sample to the system. Using a nebulizer and a spraychamber the liquid is converted into an aerosol, which is then introduced into the centre of a hot plasma causing it to dry, decompose and then atomize. The atoms are excited and emit light at characteristic wavelengths dependent on the element as they return to lower energy states. The emission from the plasm is detected and the

concentration of an element is quantified by comparing its emission to that of known concentrations from element standards plotted on a calibration curve.[40]

The analysis was done using an Agilent 4210 MP-AES Optical Emission Spectrometer, with an Agilent SPS 4 Autosampler. Four calibration standards were made at concentrations of 0.1, 0.5, 1 and 10 mg/L.

Sample preparation

Synthesis was done according to the method described in section 2.2.2, but with a slightly different procedure for washing to ensure that all the NPs were included in the analysis. The first washing was carried out as explained before, while the second wash ing was done using a Minispin at 14500 rpm for 20 minutes. By doing this, it was easier to remove more supernatant while not losing AuNPs. The samples were then weighted to 6 g during dilution.

Because of organics in the solution possibly being damaging for the plasma torch, a low concentration was desired. Method detection limit (MDL) for Au in geological samples was reported to be between 1.8 - 7.2 ppb by various sources[40] [42], but nevertheless measured at ppm-levels. Back-calculations were done based on Au-values detected in the case of AuNPs by others on MP-AES.[43], and found to be at the lowest 300 ppb. Based on this, Au was diluted to a maximum of 1 ppm (theoretical highest possible concentration).

0.75 mL Aqua Regia (3:1 volume ratio HCl:HNO_3) was used to digest 10 µL of sample solution. The samples were left to digest for 2 days, and then diluted with MQ-water to a total of 5 mL.

3 Results and Discussion

The results of the experiments conducted in this work are presented and discussed in this section. Analysis was done using mainly UV-Vis and S(T)EM. The results were compared closely to what was found by Raghunathan et al.[1] and to the project leading up to this work.[2]

In the first part, Tannic Acid was used to replace Ascorbic Acid as the reducing agent. A screening design was made to explore several factors at once. The amounts of OA, $AgNO_3$ and TA were varied along with the pH. S(T)EM images and a mathematical model obtained from the design are presented.

In the second part, the effects of pH and OA (related to previous work[1] [2]) were explored. First, the pH was increased to 11 at the beginning of the synthesis. Then, the amount of co-surfactant was increased to 200 µL OA for some experiments. Then, experiments where the pH was changed to 11 directly before adding AA are presented and compared to results found by Raghunathan et al.[1] The ions involved at 0, 20 and 200 µL OA were studied more closely to observe the effect of this compared to the pH. Finally, a yield study of three syntheses is presented, followed by a discussion on the growth mechanism.

3.1 Varying additives

It was of interest to explore a different reducing agent, and Tannic Acid was chosen. As described in section 1.5.4, TA is a much larger molecule than AA, and may give different results when reducing Au.

3.1.1 Experiment design

To get a quick overview of the effects with TA, a design of experiments (DOE) was made using JMP software. The design used was a screening design where the minimum and maximum values for the parameters involved were chosen. Four factors were chosen and varied according to knowledge obtained from previous work and literature. The factors and their ranges are summarized in Table 3, followed by explanations below.

Table 3: Factors used in screening design for Tannic Acid.

Factor	**Min**	**Max**
Oleic Acid	0 µL	100 µL
$AgNO_3$	150 µL	1500 µL
pH	1.5	11
Tannic Acid	100 µL	1650 µL

OA: The co-surfactant Oleic Acid was of interest as it gave characteristic forms when used with AA (as seen in literature[1] and my earlier work[2]). The upper limit was set to 100 µL to understand its dual role as reducing agent and co-surfactant.

pH: The pH minimum limit was set to the lowest pH-value (pH 1.5) used in previous work leading up to this work.[2] [1] The highest value explored in the previous work was pH 10. In the current experiments the highest pH was set slightly higher, at pH 11. The pH was adjusted before adding TA in these experiments.

TA: The amount of TA was based on results presented by another member of the group[44], where the amounts of TA (0.1 M) were varied in the AuNP synthesis. The minimum amount was set to 100 µL, and the upper value to 1650 µL.

$AgNO_3$: As mentioned in 1.5.4, TA has been used in other variants of AuNP syntheses, so the molar ratio of $AgNO_3$ was calculated from these and adapted to the system explained in 2.2 for this project. Ag is known to affect the AR, so to determine the range to be used a set of experiments were conducted. Six experiments with varying amounts of 4 mM $AgNO_3$ between 0.15 - 3.00 mL were carried out. UV-Vis results from these are displayed in Figure 20.

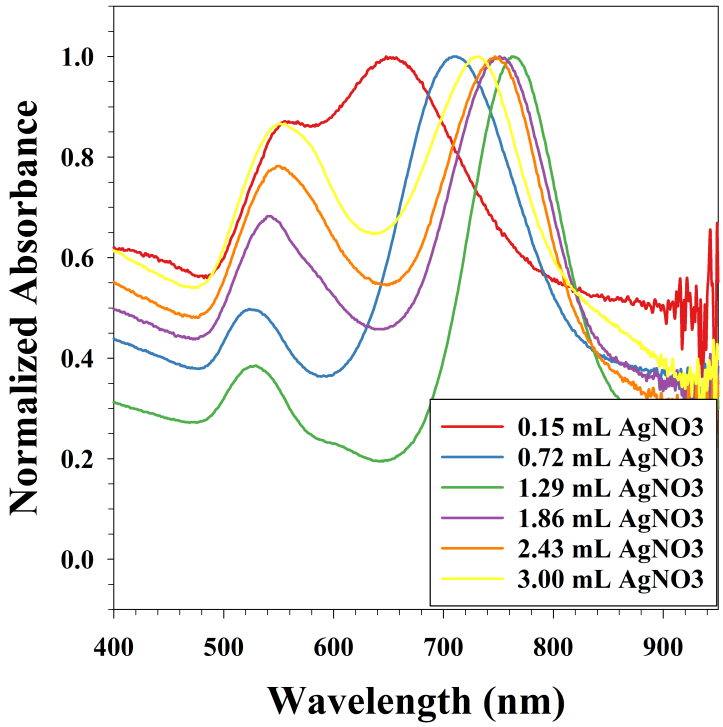

Figure 20: UV-Vis spectra of AuNPs synthesized with TA, with varying amounts of $AgNO_3$.

From the UV-Vis, it could be seen that the AR was likely at the highest when 1.29 mL $AgNO_3$ was used, and decreasing from there. To check this hypotheses, four of the samples were imaged and measured in S(T)EM. These images are displayed in Figure 21.

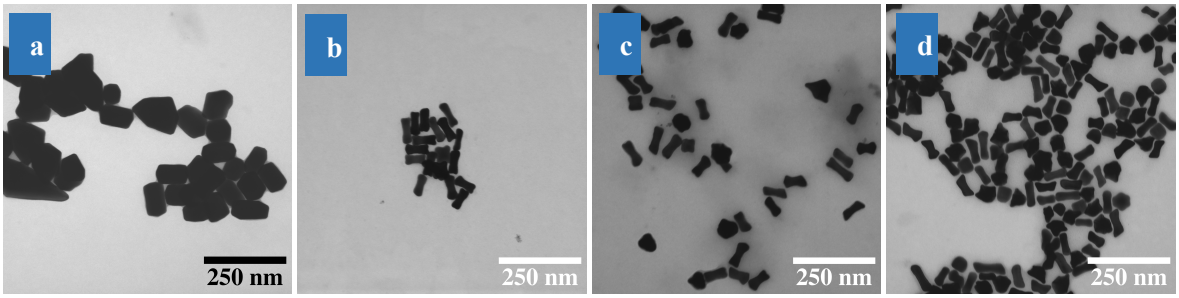

Figure 21: AuNPs synthesized using Tannic Acid, with varying amounts of $AgNO_3$. a) 0.15 mL, b) 1.29 mL, c) 1.86 mL, d) 3.00 mL.

Image a in Figure 21 displays the large bottom product obtained with 0.15 mL $AgNO_3$, this sample did not have a separate top product. Figure 21b, c and d show the smaller etched rods obtained at the higher amounts of Ag. The lengths and ARs are listed in Table 4.

Table 4: Length (L) and aspect ratio (AR) of AuNPs with TA and varying amounts of $AgNO_3$.

$AgNO_3$ (mL)	**L (nm)**	**AR (nm)**
0.15	111 ± 58	1.5 ± 0.4
1.29	64 ± 8	3.1 ± 0.8
1.86	63 ± 11	2.5 ± 0.9
3.00	55 ± 11	2.1 ± 1.0

The ARs from the measurements confirmed what was seen from the UV: the AR was at the lowest at 0.15 mL, and highest at 1.29 mL $AgNO_3$. The AR also decreased when increasing the amount of $AgNO_3$ above 1.29 mL. The range for $AgNO_3$ was chosen to be 0.15 to 1.50 mL for the design. This complies with what was mentioned in section 1.5.3 about the AR being increased with higher concentrations of $AgNO_3$, but only up to a certain concentration. [28]

When introducing the factors along with maximum and minimum limits to the JMP software, Table 5 was obtained. This lists the experiments carried out and their numbering. The responses of interest were set to be length and AR.

Table 5: Tannic Acid design of experiments, definite screening analysis.

#	**block**	**OA (µL)**	**AgNO3 (µL)**	**pH**	**TA (µL)**
1	1	0	825	11	100
2	1	100	150	1.5	100
3	1	0	150	6.25	100
4	1	0	1500	11	1650
5	1	100	1500	6.25	1650
6	1	100	825	1.5	1650
7	1	50	825	6.25	875
8	2	100	150	11	875
9	2	100	1500	11	100
10	2	0	150	1.5	1650
11	2	0	1500	1.5	875
12	2	50	1500	1.5	100
13	2	50	150	11	1650

3.1.2 Results and output

To obtain the lengths and ARs of the particles produced in this study, S(T)EM images were captured and processed. Four of the experiments did not give any product and were not analysed further. It should be noted that pH 6.25 was challenging to obtain precisely, as the pH changed rapidly with very small amounts of NaOH when raised from ~3. However, the pH obtained was close, and a smaller change in the pH was assumed to not affect the results significantly. The pH values were left at 6.25 in the software, as the software did not give a fit if these were changed. S(T)EM images are presented in Figure 22 along with UV-Vis-spectra as icons in the bottom left corner.

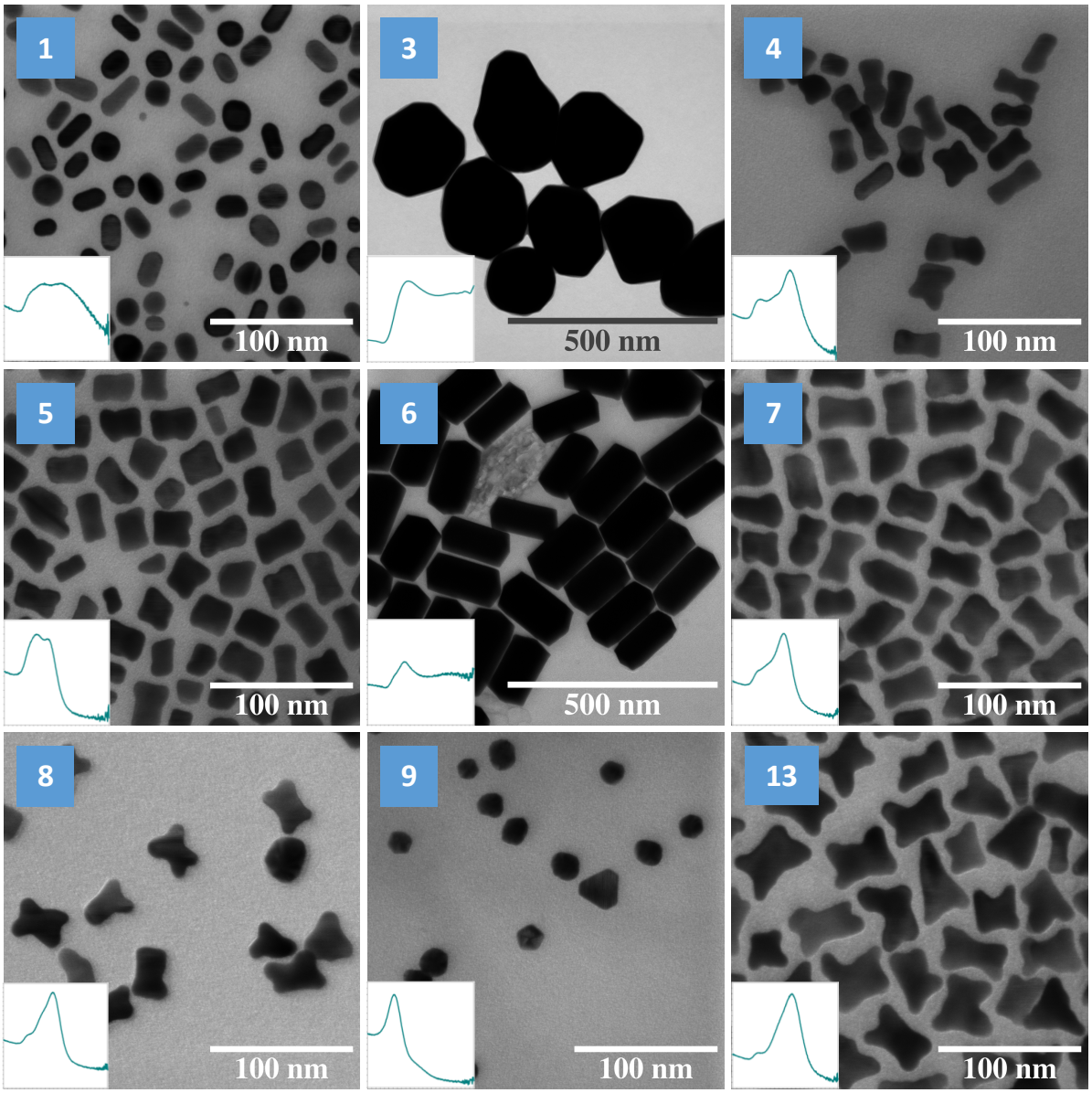

Figure 22: S(T)EM images from TA DOE. Numbered by number name (can be found in table). UV-spectra are normalized and plotted from 400 - 900 nm for each sample.

Experiments #3 and #6 in Figure 22 yielded only large particles that had precipitated to the bottom during growth. These gave no top product, and UV-Vis of the supernatant verified this.

Experiments #4, #5 and #7 gave similar-looking shapes; etched particles/rods with low AR. Shapes from #8 and #13 were also similar to these, but generally less rod-shaped with more growth of the etched part. #9 gave mostly rounded shapes or other shapes with AR = 1. #1 gave small rods and some spheres.

Experiments 2, 10, 11 and 12 are not included in Figure 22, as these gave no product. Before washing the samples, 10 and 11 were yellowish in colour, while 2 and 12 were completely blank. A picture of these in the centrifuge tubes is shown in Figure 23.

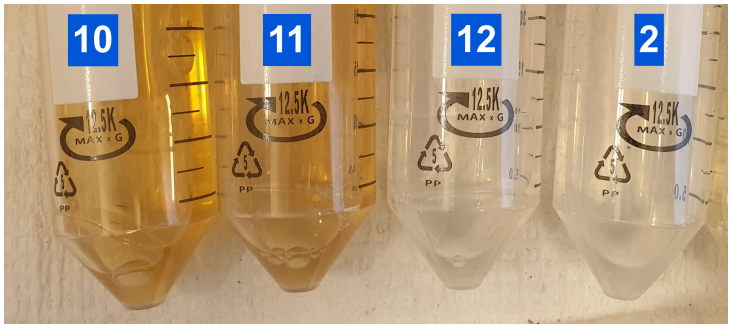

Figure 23: Experiment solutions of samples that gave no product.

The lengths and AR-values for the experiments that gave some product are given in Table 6.

Table 6: Results from TA DOE

#	Length (nm)	AR	UV peaks
1	23 ± 4	2.0 ± 0.7	592, 671
3	238 ± 49	1.3 ± 0.2	583.5
4	31 ± 6	2.3 ± 0.7	535, 679
5	26 ± 5	1.7 ± 0.4	554, 607
6	180 ± 27	1.9 ± 0.3	573
7	33 ± 6	2.1 ± 0.5	642
8	34 ± 6	1.9 ± 0.4	635
9	19 ± 3	1.2 ± 0.2	525
13	40 ± 8	2.0 ± 0.5	524, 683

L and AR from Table 6 were used in the screening analysis. Experiments that gave no product were considered to have both length and AR of 0, as expected by the software. Figure 24 shows the predicted plots for the length and AR given by the software for the fit.

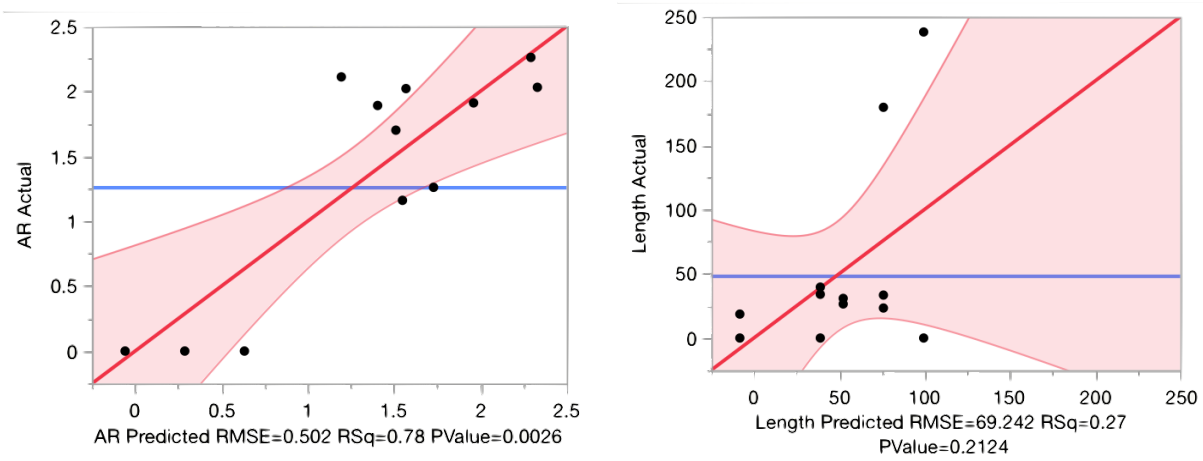

(a) (b)

Figure 24: Predicted plots given by JMP for a) Aspect ratio (AR) and b) length.

The fit gave a linear trend for the AR (Figure 24a), with an R^2 value of 0.78, while the prediction of length (Figure 24b) gave a low R^2 of 0.27. Equation 5 gives a formula that can be used to calculate the predicted AR based on the design.

$$\begin{aligned}\text{Aspect Ratio} =& 1.0506673227 + 0.7632203513 \cdot \left(\frac{\text{pH} - 6.25}{4.75}\right) \\ &+ 0.3455599841 \cdot \left(\frac{\text{TA} - 875}{775}\right) + 0.004297477 \cdot \text{Length}\end{aligned} \tag{5}$$

In this equation, "TA" denotes the amount of tannic acid in µL, and "pH" is the pH value. Here, the length is also considered to be a factor.

3.2 Effect of parameters using Tannic Acid

All the four experiments without product were at the lowest pH of 1.5. Even though the other parameters were varied, the low pH affected the reaction and resulted in no products which points towards the other parameters having less effect at this low pH. The low pH can cause the reduction potential to be low, and hence the reaction would need more TA for a sufficient reaction, which is seen in #6. Despite having a low pH, #6 had the maximum amount of reducing agent(s): 100 µL OA and 1650 µL TA and therefore it gave product. The NPs obtained in experiment #13 bear a resemblance to the branched particles obtained at high pH (11.5) with AA by Wu et al.[33] (see section 1.5.5).

From the fit given by the predicted plot and equation, it seems that pH had the most effect on the AR. The prediction of L was not as accurate. It should however be taken

into consideration that the software didn't allow empty or N/A as values for the screening fit. The value of 0 for L and AR when no product was obtained could skew the results and give a more linear fit (0-values seen at the bottom of the plot in Figure 24a).

The results of this DOE could imply that there are not clear trends for variations of these parameters combined or that a larger DOE should be considered to give more accurate predictions. The interplay of the varied parameters makes it complicated to derive the direct effect of the parameters individually. However, the pH seemed to have the most effect on the outcome as pH 1.5 often gave no product, while there was consistently some product for the other experiments at pH 6.25 and 11. Because of this, the pH was explored further, but with the more commonly used reducing agent AA. In the remaining sections, only AA is used.

3.3 High pH at the start

As seen in the previous sections, the pH is an important criteria for the growth, so this was studied further with AA as the reducing agent. In my previous work[2] the pH was changed at the start of the synthesis. pH-values up to 10 were analyzed for three synthesis variations: without silver, with silver and with silver plus 20 µL OA. When Ag was present in the solution, the AuNRs at pH 1.5, 3 and 6 showed an increase in length with increasing pH. However, the length decreased when the pH was further increased to 10. This was also evident in the kinetics, where an increase in pH up to pH 6 led to a higher growth rate, but at pH 10 it was slower. The same trend in the kinetics was seen for experiments with 20 µL OA and without Ag as well. A higher pH was desired to see if the trends continued, and so a pH of 11 was studied in this work. To decouple the effects of OA and the role it plays in affecting the pH and/or acting partly as a reducing agent, experiments looking at the effect of a high amount of OA (200 µL) were also conducted. This was studied at pH 1.5, 3, 6 and 10.

UV-Vis spectra of AuNPs synthesized with a starting pH of 11 are shown in Figure 25, and the values of the LSPR-wavelengths are listed in Table 7. Values for synthesis at pH 1.5, 3, 6.1 and 10 are also included for comparison purposes.

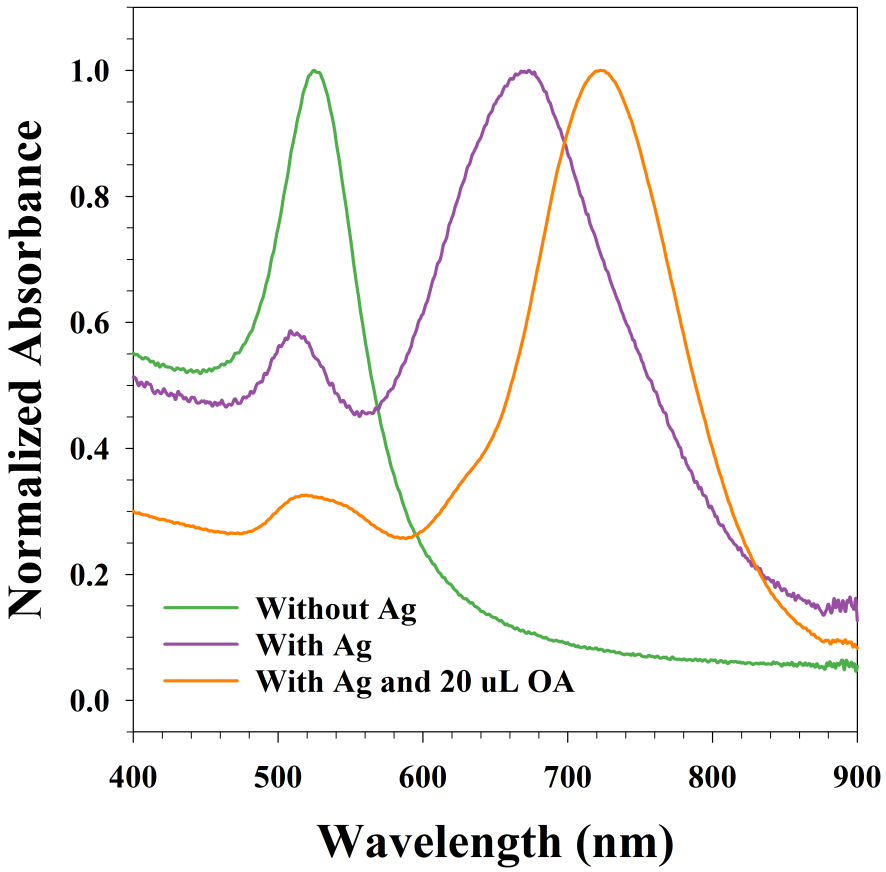

Figure 25: UV-spectra for AuNPs synthesized with starting pH of 11.

Table 7: LSPR-wavelengths of AuNPs at various synthesis conditions and pH-values.

Sample	**Starting pH**	**LSPR**
Without $AgNO_3$	1.5	537
	3	535
	6.1	532
	10	533
	11	525
With $AgNO_3$	1.5	512, 679
	3	509, 772
	6.1	507, 793
	10	517, 677
	11	509, 673
With $AgNO_3$ & 20 µL OA	1.5	514, 736
	3	520, 730
	6.1	520-600, 695
	10	530, 727
	11	519, 732

The absorbance spectra at pH 11 in Figure 25 show similar characteristic shapes as were typically observed at lower pH as well.[2] Differences are seen in where the peaks are located, as listed in Table 7. For AuNPs without silver, the LSPR peak generally shifts slightly to the left with increasing pH. When silver is present, there is no clear trend in where the LSPR wavelengths are found. However, the distance from the transverse to the longitudinal peak is greatest at pH 6.1 and 3. With 20 µL OA, the distances between the peaks are similar to each other (apart from at pH 6.1), though the peaks are shifted.

Synthesizing particles with 200 µL OA resulted in two products; top and bottom. UV-Vis spectra of these particles synthesized at pH 1.5, 3, 6 (no change in pH) and 10 are shown in Figure 26. The LSPR-wavelengths are listed in Table 8

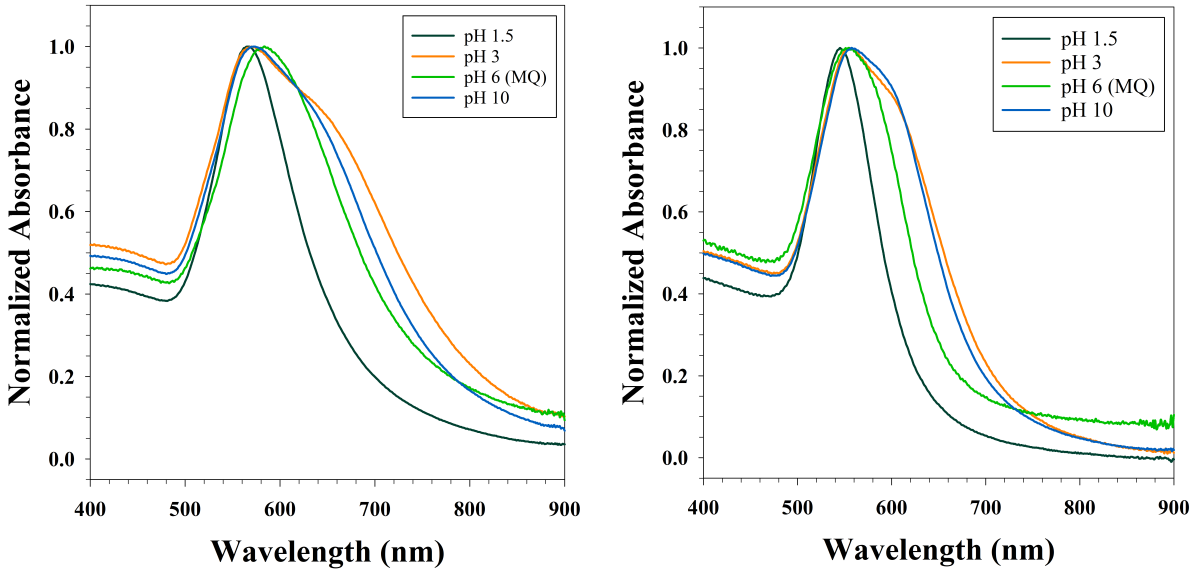

(a) Bottom product

(b) Top product

Figure 26: UV-spectra of AuNPs synthesized with 200µL OA.

Table 8: LSPR-wavelengths for bottom and top products of synthesis with 200 µL OA.

Type of product	**Starting pH**	**LSPR**
Bottom product	1.5	565.5
	3	570
	6.1 (MQ)	583
	10	573
Top product	1.5	545
	3	557
	6.1 (MQ)	554
	10	557

All the products of the AuNPs with 200 µL OA have similar UV-Vis spectra, though the top products have a slightly narrower and more blue-shifted peak than the bottom products.

The effects of pH on the AuNPs' shapes were observed by S(T)EM images. Images j-l in Figure 27 display the shapes obtained when altering the starting pH to 11. The remaining images (a-i) are from previous work[2], and are displayed to compare with the current results.

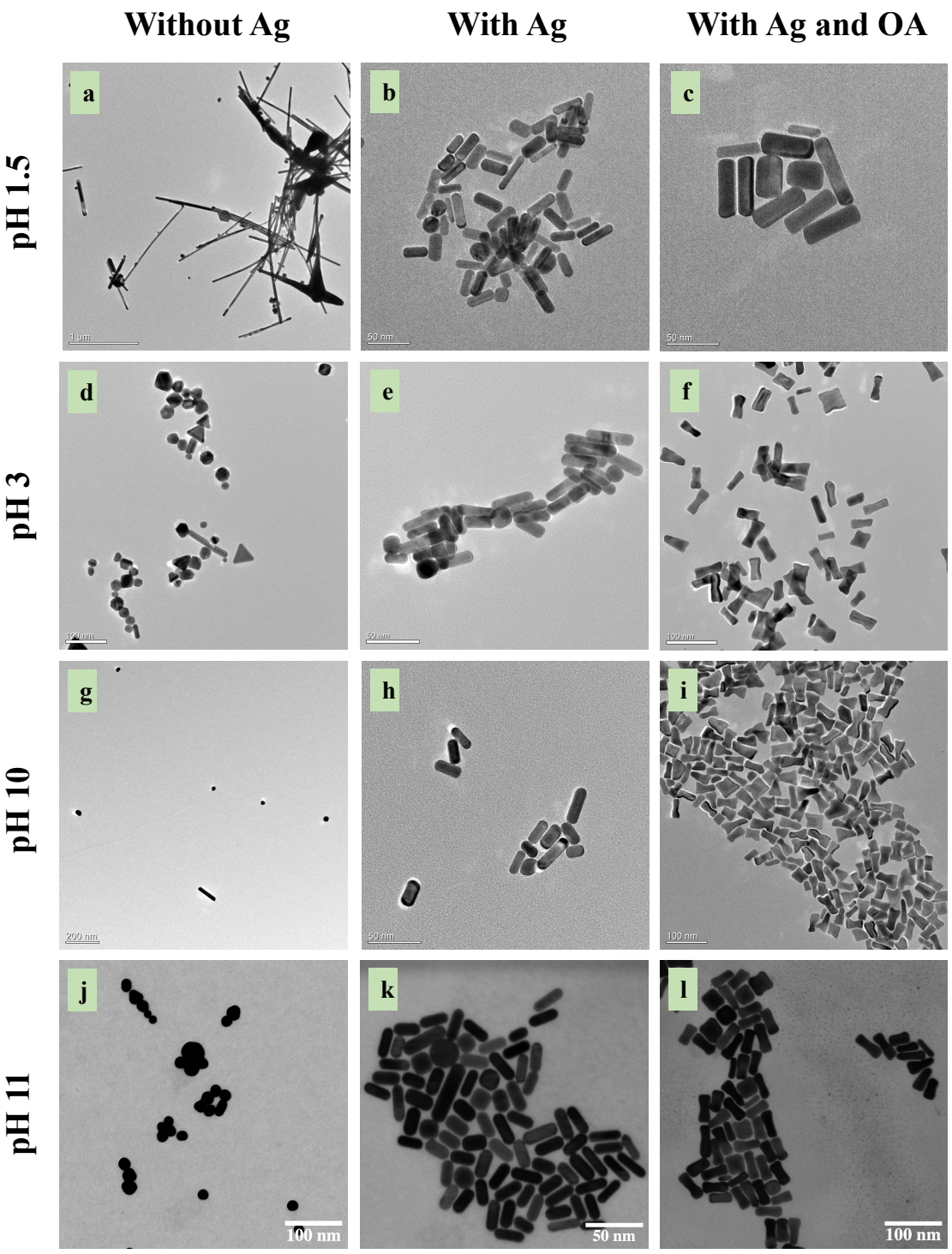

Figure 27: Effect of pH on the shape of AuNPs. (a–l) Representative TEM[2] and S(T)EM images of different AuNPs.

The shapes of the particles at pH 11 were not very different from those at pH 10. Synthesis without Ag resulted in mostly spherical particles of different sizes for both the highest pH syntheses (27 g,j), as well as some rods at pH 10. When Ag was present, there were mostly rods and sometimes spheres (h,k). With Ag and 20 µL OA there were etched rods at both pH 10 and 11 (i,l).

Table 9 lists the average length and AR of each sample obtained by manual measurements of the images, using ImageJ.

Table 9: Average length and aspect ratio (AR) for manually measured AuNPs from S(T)EM images.

Sample	**Starting pH**	**Length (nm)**	**AR**
Without $AgNO_3$	1.5	483 ± 554	-*
	3	30 ± 10	1*
	10	35 ± 23	1.3 ± 1.1
	11	18 ± 5	1*
With $AgNO_3$	1.5	31 ± 6	2.8 ± 1.0
	3	37 ± 9	3.7 ± 0.9
	6†	40 ± 8	3.2 ± 1.0
	10	26 ± 6	2.5 ± 0.6
	11	23 ± 5	2.3 ± 0.7
With $AgNO_3$ & 20 µL OA	1.5	53 ± 10	3.5 ± 1.0
	3	48 ± 9	2.9 ± 0.7
	6†	44 ± 6	2.9 ± 0.9
	10	43 ± 8	2.9 ± 0.8
	11	40 ± 6	2.8 ± 0.8

The measured sizes reveal that smaller particles were obtained at a higher pH when no $AgNO_3$ was present. When $AgNO_3$ was present, smaller size and lower AR were obtained. The same trend is seen for AuNPs synthesized with 20 µL OA.

*NPs synthesized without $AgNO_3$ gave indistinguishable nano wires (pH 1.5), or shapes with the same long and short axis lengths (pH 3 and 11).

† Milli-Q water was used in the syntheses from a previous paper [1] (from the same lab), and the pH is assumed to be ∼ 6.

All the experiments with 200 µL OA resulted in similar particles with low kinetics and hence an experiment at pH 11 was not performed. They all had separate top- and bottom products, and yielded mostly tetrahexahedra (THH) shapes for both of these products. Sizes of the particles obtained for 200 µL OA are listed in Table 10.

Table 10: Average length and aspect ratio (AR) for manually measured AuNPs from S(T)EM images. Particles synthesized with 200 µL OA.

Type of product	Starting pH	Length (nm)	AR
Bottom product	1.5	90.9 ± 15.2	1.1 ± 0.1
	3	108.5 ± 18.4	1.5 ± 0.3
	6.1 (MQ)	111.1 ± 14.7	1.3 ± 0.1
	10	108.6 ± 15.1	1.3 ± 0.3
Top product	1.5	60.0 ± 12.0	1.1 ± 0.1
	3	79.0 ± 16.6	1.4 ± 0.3
	6.1 (MQ)	65.5 ± 17.2	1.3 ± 0.3
	10	65.9 ± 16.9	1.3 ± 0.4

All the bottom products were similar in size to each other, and so were the top products. The aspect ratios are also close to each other for all the products, and the only difference seen is that the top product yields smaller sizes than the bottom product. The shapes of the particles obtained at 200 µL OA also had the same shapes, and an example from the S(T)EM images can be seen to the right in Figure 28.

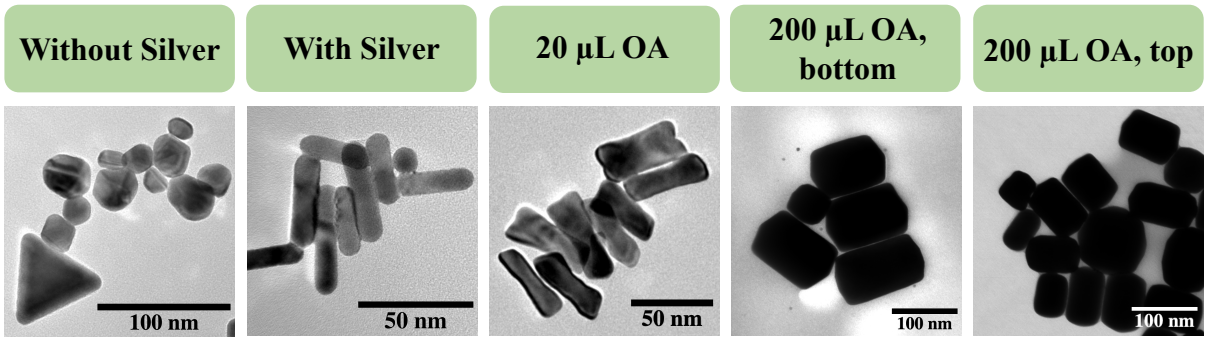

Figure 28: Change of shape with varying synthesis parameters at pH 3.

Figure 28 displays the change of shape with varying synthesis parameters at pH 3, which is representative for most of the other pH-values. From the figure it can be seen that mostly rounded particles/ particles with AR = 1 are formed when no silver is present. When silver is added, rods are obtained. By adding a small amount of OA, the rods are etched. By increasing the amount of OA to 200 µL, the particles grow much larger and are shaped as THH.

3.3.1 Kinetics

The growth rates at pH 11 (starting-pH) were measured for the 3 first synthesis variations and are shown in Figure 29 and listed in Table 11. The graph and table also show the values from literature[2] [1] which have the values for lower pH. Kinetics of experiments with 200 µL OA from the current work are also included for pH 3, 6 and 10. pH 1.5 was not included because it was too slow for the instrument.

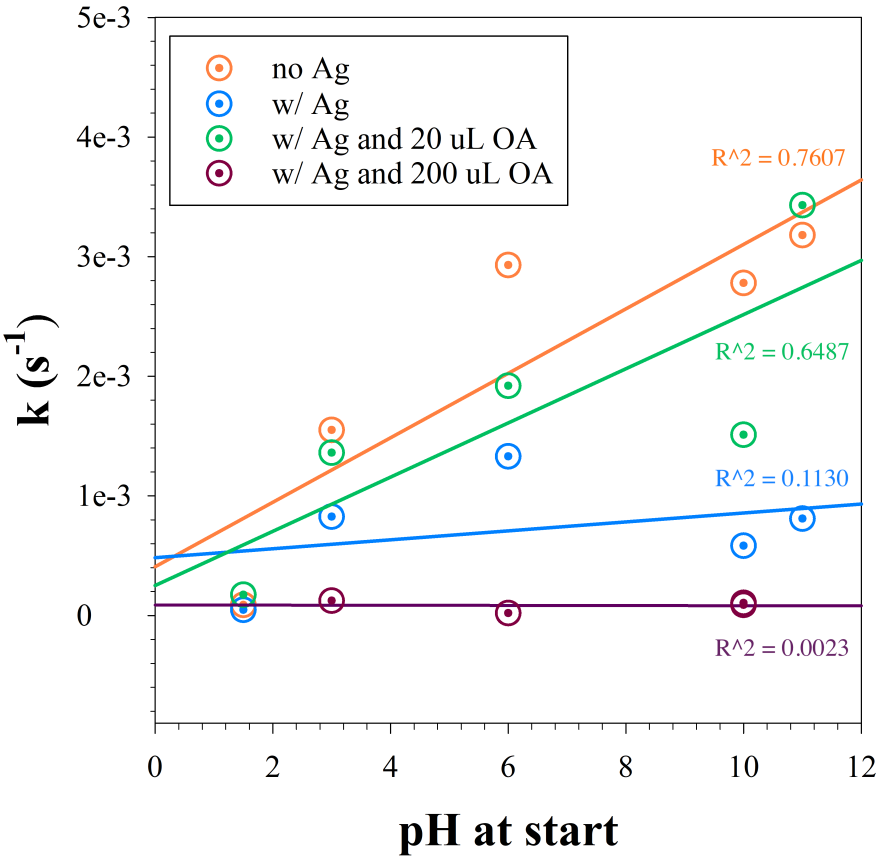

Figure 29: Growth rates (k) for four synthesis variations at different pH-values.

Within each category of experiments, the growth rate (k) increases when pH is increased up to 6. When increasing the pH further, the growth rates don't follow the same trend of increasing with increasing pH. Within each category, there is a drop in k at pH 10, before the rate again increases at pH 11. The values before adding AA are also displayed in Table 11, as these could affect the reduction potential of AA, and thus could also be related to the growth rate.

Table 11: Growth rate (k) for each of the sample conditions.

Sample	**Starting pH**	**pH before AA**	**Growth rate, k (s^{-1})**	R^2
Without $AgNO_3$	1.5	1.8	$8.85 \cdot 10^{-5}$	0.9990
	3	3.0	$1.55 \cdot 10^{-3}$	0.9991
	6*	3.6	$2.93 \cdot 10^{-3}$	
	10	3.5	$2.78 \cdot 10^{-3}$	0.9999
	11	4.1	$3.18 \cdot 10^{-3}$	0.9985
With $AgNO_3$	1.5	1.7	$4.70 \cdot 10^{-5}$	0.9996
	3	3.1	$8.26 \cdot 10^{-4}$	0.9998
	6*	3.6	$1.33 \cdot 10^{-3}$	
	10	3.4	$5.83 \cdot 10^{-4}$	0.9998
	11	5.1	$8.09 \cdot 10^{-4}$	0.9998
With $AgNO_3$ & 20 µL OA	1.5	1.7	$1.73 \cdot 10^{-4}$	0.9988
	3	3.1	$1.36 \cdot 10^{-3}$	0.9989
	6*	3.4	$1.92 \cdot 10^{-3}$	
	10	3.2	$1.51 \cdot 10^{-3}$	0.9991
	11	3.6	$3.43 \cdot 10^{-3}$	0.9980
With $AgNO_3$ & 200 µL OA	3	2.7	$1.24 \cdot 10^{-4}$	0.9840
	6.1	2.9	$2.00 \cdot 10^{-5}$	0.9962
	10	2.9	$1.05 \cdot 10^{-4}$	0.9995

*Milli-Q water was used in the syntheses from a previous paper, and the pH is assumed to be ~ 6.

3.4 High pH before addition of reducing agent

For syntheses without Ag, with Ag and with 20 µL OA the pH was changed at a later step in the synthesis to see if this had a different effect on the final AuNPs. This is an extension of the previous work by Raghunathan et al. [1], where the pH was changed before addition of AA up until pH 10. As the pH at the start was increased to 11 in previous experiments of the current work, the effect of pH 11 before adding AA was of interest to allow for further understanding of the role of pH. UV and S(T)EM were used to analyze the resulting particles. These results differed from those where the pH was adjusted at the very beginning. Figure 30 displays the UV-spectra of the particles obtained for these conditions.

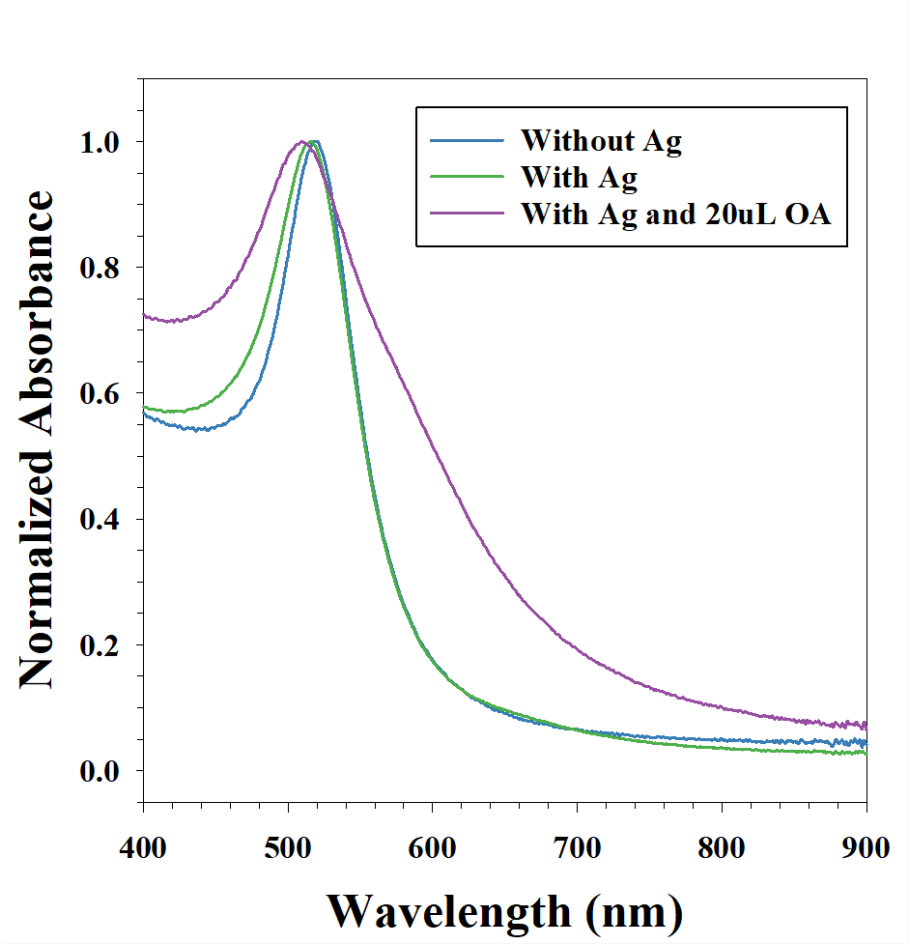

Figure 30: UV-spectra for AuNPs synthesized at pH 11 before adding AA.

With and without Ag display similar peaks at wavelengths 516 nm and 519 nm, respectively. When 20 µL OA was present the LSPR peak is at 509 nm and is broader than the two others.

Figure 31 shows the shapes obtained for AuNPs synthesized at pH 11 before adding AA.

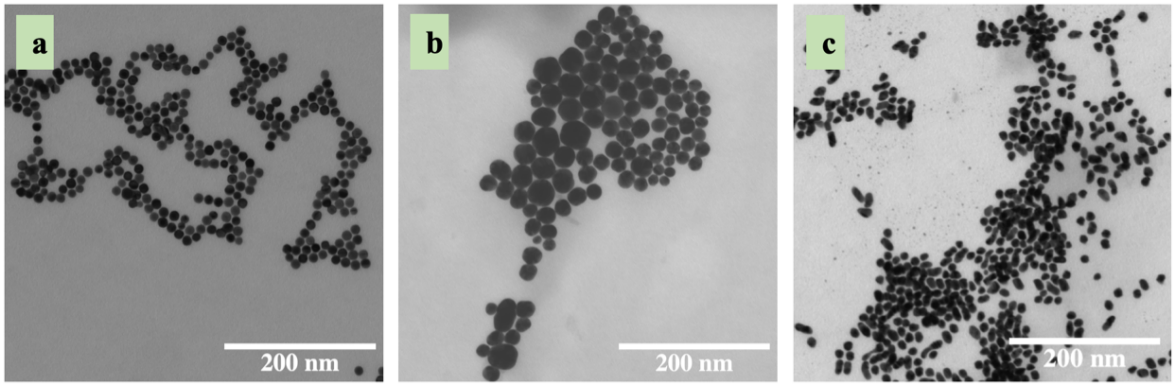

Figure 31: TEM and S(T)EM images for NPs synthesized when adjusting pH to 11 before adding AA: (a) without $AgNO_3$, (b) with $AgNO_3$ and (c) with $AgNO_3$ and 20µL OA.

All the synthesis variations at pH 11 yielded mostly spheres. When no Ag was present the spheres were uniform (Figure 31a), when Ag was present the spheres were more varying in size (Figure 31b), and with Ag and 20µL OA the particles looked more like tiny rods (Figure 31c). This is different from what was seen in the paper. At pH 10, particles without Ag gave varying shapes (including some rods), particles with Ag gave etched NPs and particles with 20 µL OA gave varying shapes.[1] Table 12 lists the average lengths and ARs for the three variations at pH 10 (from literature[1]) and 11.

Table 12: Average length and aspect ratio (AR) of AuNPs synthesized at pH 10 and 11 before AA. Measurements from S(T)EM images.

Sample	**Shape**	**Length (nm)**	**AR**	**LSPR**
Without $AgNO_3$, pH 10	random	36	1.8	524
Without $AgNO_3$, pH 11	spheres	12 ± 1	1	519
With $AgNO_3$, pH 10	etched	36	2.8	721
With $AgNO_3$, pH 11	spheres	25 ± 7	1	516
With $AgNO_3$ and OA, pH 10	random	18	1.1	520
With $AgNO_3$ and OA, pH 11	spheres	14 ± 4	1.5 ± 0.5	509

The sizes from pH 11 confirm what is seen from the S(T)EM images. The particles were the smallest in the sample without Ag, and largest in the sample with Ag. The AR of the particles imply that there were spheres with and without Ag, and several small rods with 20 µL OA. In comparison to those obtained at pH 10, pH 11 gave more uniform shapes with shorter lengths.

After washing the AuNPs synthesized at pH 11, the supernatant for without Ag still contained a reasonable amount of colour (see Figure A1). This implies that the solution also contained smaller particles which were not heavy enough to precipitate during the washing.

Kinetics are not listed for these AuNPs, as the particles rapidly grew before the sample could be transferred to the UV-Vis and were therefore impossible to measure. For the solution with silver, the growth started before the seed was added. This was observed by the colour changing from blank to red directly after addition of AA, before addition of seed. In the two remaining experiments, the colour change was observed directly after adding the seed.

3.5 Effect of OA and pH

This section discusses the effects of increased pH and oleic acid based on the observations from sections 3.3 and 3.4.

As shown in section 3.3, changing the pH to 11 at the beginning of the syntheses resulted in particles similar to those obtained at pH 10. The transverse LSPR wavelengths were lower than at pH 10, and for the two syntheses with silver, the distance between the two peaks was slightly greater for pH 11. A greater distance between the UV-peaks could indicate a higher AR, but the manual size-measurements suggested otherwise. 200 µL OA resulted in similar UV-spectra at all pH values, indicating similar shapes for all these.

From the shapes in Figure 27, it can be seen that there is generally less shape-control when no silver is present, as this mostly yields random or rounded shapes at all pH values. As mentioned in section 1.5.3, $AgNO_3$ plays a role in the symmetry-breaking of the AuNPs, so asymmetry is not expected without it. With silver present in the solution there are generally rods, and with 20 µL OA there are mostly etched rods for all pH values except pH 1.5. This points towards pH not having a strong influence on the shape. When it comes to size, there does not seem to be a general trend for the lengths and ARs according to pH for the samples with and without Ag. However, for the samples with 20 µL OA the average length consistently decreases with increasing pH, while the AR shows a slight decrease with increasing pH. This could be caused by the supersaturation being higher at higher pH, causing more rapid growth on the less energetically favorable facets.

When a higher amount of oleic acid (200 µL OA) was introduced to the system, another shape was obtained: tetrahexahedra. This applied to all the pH-values studied with 200 µL OA. Apart from the shapes and ARs all being similar, there were no clear trends seen as the pH was changing. This points towards OA having a more dominating effect on the final particles than the pH. Note that the variations in length could be related to which particles were measured (S(T)EM bias) and could also be affected by the varying angles these large particles were seen from.

No clear trend is seen in the data from the kinetics of the experiments with 200 µL OA. However, they all have very slow growth kinetics. For the remaining synthesis variations, the growth rate data obtained in this study implies that an increase in pH doesn't necessarily lead to a higher k-value, as might have been guessed from a previous study [2]. The k-values at starting-pH 6 (no change in pH) for no Ag, with Ag and with 20 µL OA were taken from another study carried out in the same laboratory [1], and

could therefore deviate slightly from what would have been found at this time. However, assuming that these are representative and fit in with the data obtained in the current project, they support the claim. It should be taken into consideration that there were ions added at pH 1.5, 3, 10 and 11, but not at pH 6. The ions could have an effect on the system, causing the "drop" in k-value between pH 6 and 10, before another increase in the rate from pH 10 to 11.

When changing the pH to 11 before adding AA the resulting NPs were very different from the particles synthesized at starting-pH 11. The rapid growth of these could be related to the second pK_a-value of AA, as mentioned in section 1.5.4. This rapid growth and the resulting rounded particles could point towards the pH causing a high supersaturation, making the growth too quick to obtain a controlled growth of anisotropic AuNPs. However, several low AR rods were seen when OA was present in the solution. This supports the assumption that OA has a strong effect on the system but is still affected by the high supersaturation.

From these experiments, it seems that the amount of OA had a strong effect on the growth of the AuNPs. When it comes to pH, it should be noted that different ions were added when decreasing (HCl) and increasing (NaOH) the pH. The observed variations in the trends could imply that the ions have an affect on the system beyond changing the pH. The ions could interact and take part in the reactions apart from affecting the reduction potential. It was not straightforward to decouple the effects of pH and OA from the initial experiments, so to explore the effect of the ions more closely it was of interest to explore how the *amount* of ions added to the system would affect the outcome.

3.6 Variation of ions added

A set of experiments were conducted to explore the effects of the ions further. The variation in the pH is related to the amount of HCl and NaOH that was added, which could also have a direct effect on the system. For this, different amounts of ions were added at different steps in the syntheses. The ions were added either at the beginning of the synthesis, or directly before adding AA. The amounts of ions added were as follows:

1) 100 µL 0.5 M HCl
2) 50 µL 0.5 M HCl
3) 50 µL 0.25 M NaOH
4) 100 µL 0.25 M NaOH

These variations of ions were explored with 3 different amounts of co-surfactant; 0, 20 and 200 µL OA. The resulting products from this study were studied through pH-measurements, UV-Vis and S(T)EM.

Figure 32 displays UV-Vis spectra of the particles from this study, and Table 13 lists the LSPR-peaks. The spectra are sorted by the acidity of ions added, starting with the highest amount of acidic ions (100 µL 0.5 M HCl)(32a), and ending with the highest amount of basic ions (100 µL 0.25 M NaOH)(32d). Ions added at the start are denoted by dotted lines, while ions added before AA have solid lines. Note that all the spectra for 200 µL OA in figures 32a-d are of the top products, as all the bottom products displayed similar spectra when normalized. They all had one broad peak at 610-627 nm (see section A.6).

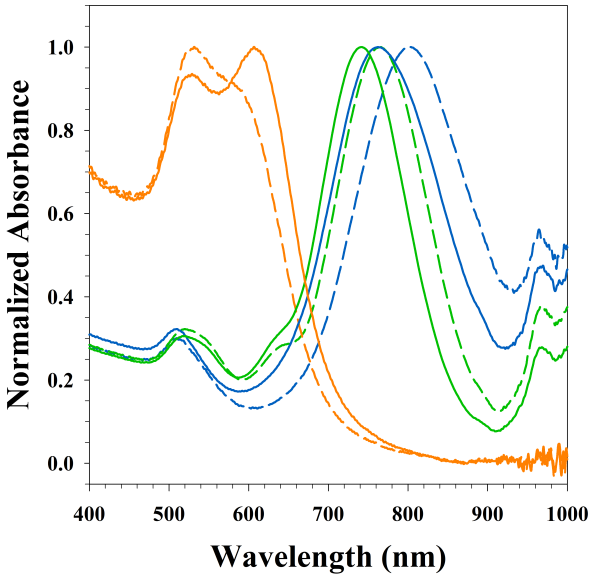

(a) 100 µL 0.5 M HCl

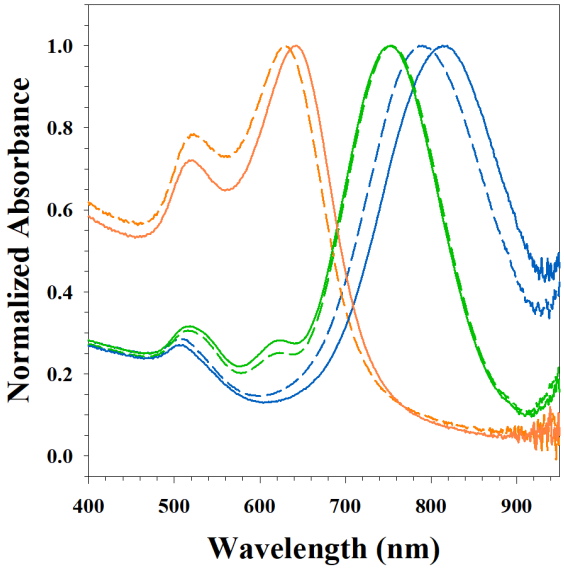

(b) 50 µL 0.5 M HCl

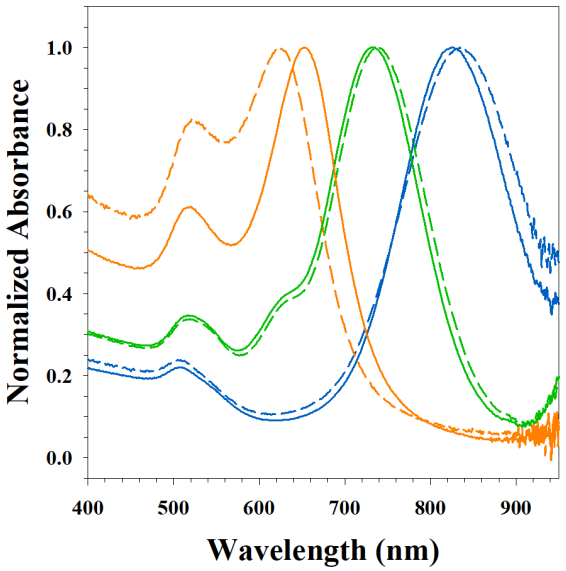

(c) 50 µL 0.25 M NaOH

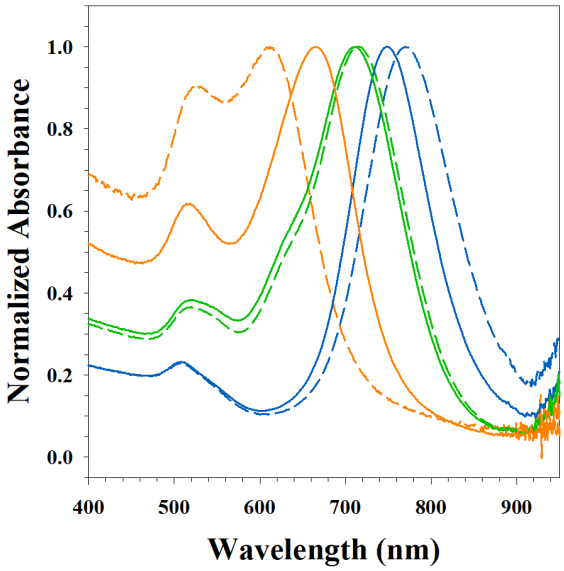

(d) 100 µL 0.25 M NaOH

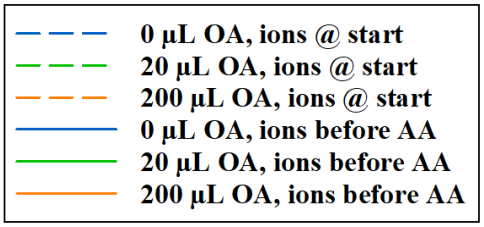

Figure 32: UV-Vis of ions study, sorted by ions. Legends at bottom are the same for all the plots. Spectra of 200 uL are of the top products.

Table 13: LSPR-wavelengths of AuNPs synthesized with varying amounts of ions added at the start of the synthesis (1) or before adding AA (2). Values listed for 200 µL are from the top product.

Ions	OA (µL)	ions added	pH before AA	UV peaks
100 µL 0.5 M HCl	0	1	3.2	510, 803, 964
	0	2	3.3	510, 763, 969
	20	1	3.2	520, 766, 966
	20	2	3.2	517, 742, 968
	200	1	2.9	532
	200	2	2.9	529, 607
50 µL 0.5 M HCl	0	1	3.3	507, 790
	0	2	3.5	510, 813
	20	1	3.2	516, 754
	20	2	3.4	518, 752
	200	1	2.9	520, 630
	200	2	3.1	521, 643
50 µL 0.25 M NaOH	0	1	4.1	505, 834
	0	2	4.4	510, 826
	20	1	3.6	519, 738
	20	2	3.7	517, 732
	200	1	2.9	523, 629
	200	2	3.2	520, 653
100 µL 0.25 M NaOH	0	1	6.2	505, 769
	0	2	7.5	508, 748
	20	1	3.9	519, 716
	20	2	4.2	522, 712
	200	1	3.0	521, 623
	200	2	3.2	514, 665

The UV-Vis spectra in Figure 32 display only slight differences between the two times of adding ions. For 0 and 20 µL OA, there are only slight shifts within each category of ions. Particles with 50 and 100 µL NaOH(Figure 32c,d) and the ones with 100 µL HCl(Figure 32a) added at the start result in slightly more redshifted longitudinal peaks (peaks at wavelenght ∼700-850nm). The opposite was observed for 50 µL HCl without OA. Top-product particles for 200 µL OA deviate from this. They display the greatest difference between the transverse- and longitudinal LSPRs when ions were added before AA. Another trend to be noted is that the increasing amount of OA causes a blueshift of the longitudinal LSPR for all the ions.

Similar UV-spectra point towards similar particles, so all the particles were imaged for ions added before AA, but only some for ions added at the start. Shapes of the AuNPs yielded when ions were added before AA are displayed in Figure 33. Note that bottom products are displayed for 200 µL OA in Figure 33, while the top products are shown in Figure 34.

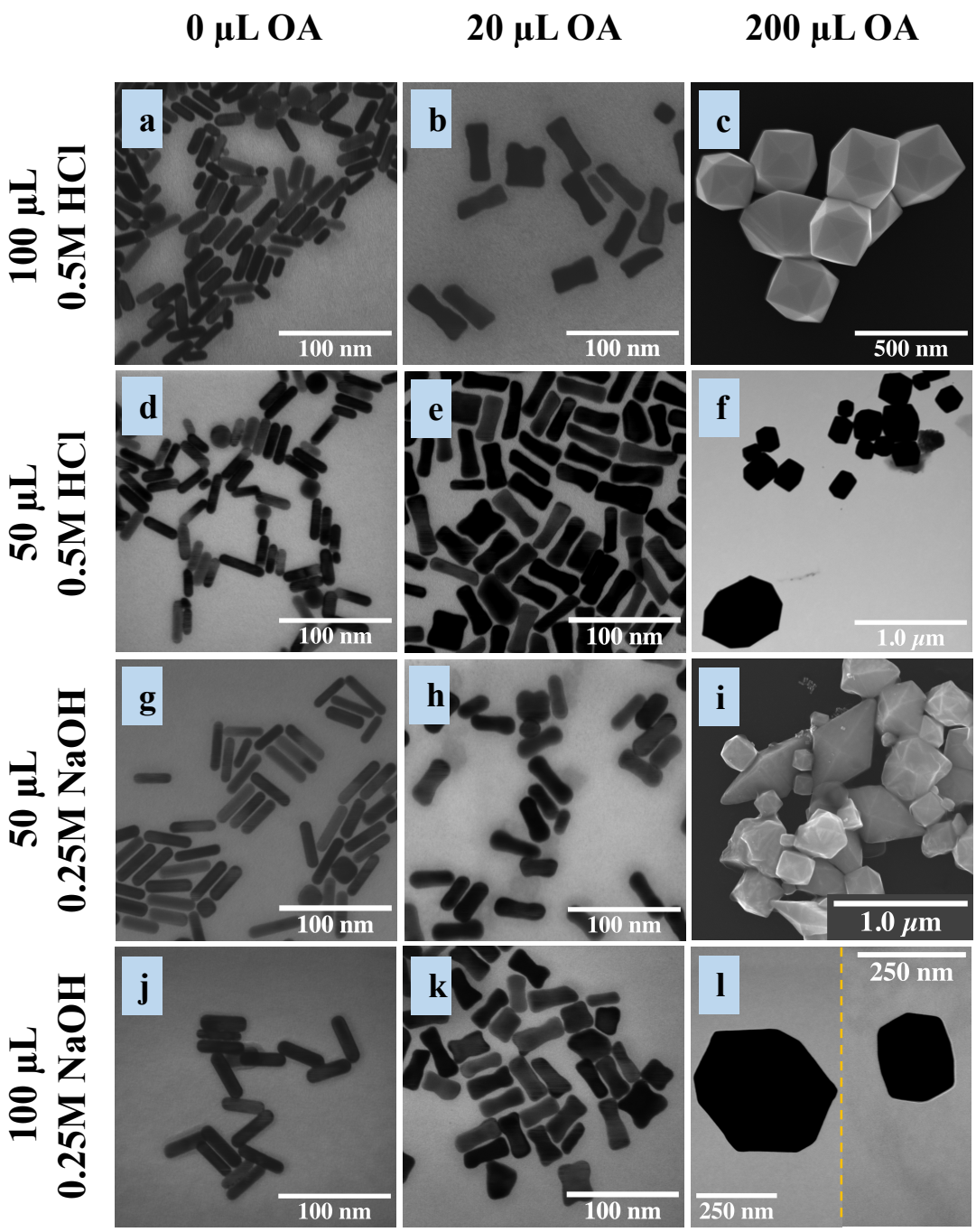

Figure 33: S(T)EM images from ions study (ions added before AA). Bottom products are displayed for 200 µL OA.

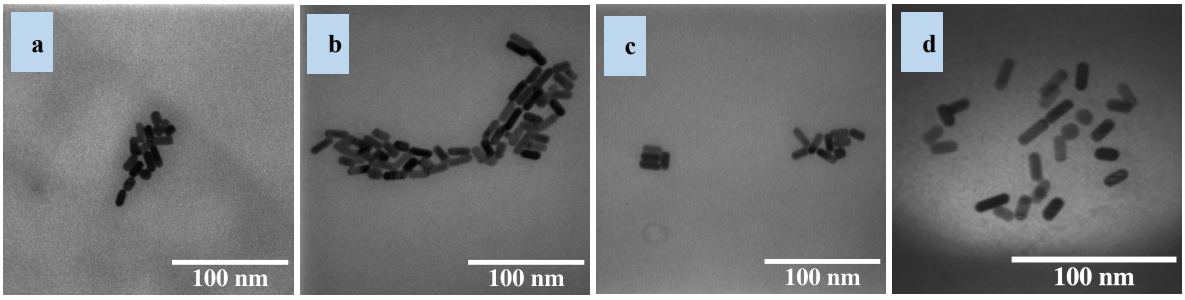

Figure 34: S(T)EM images from top product of the 200 µL OA samples with "ions before AA". 0.5 M HCl: a) 50 µL, b) 100 µL and 0.25M NaOH: c) 50 µL, d) 100 µL.

Average lengths and ARs are listed for AuNPs where ions were added before AA in Table 14.

Table 14: Length and AR for AuNPs when ions were added before AA. 200 µL has 2 products; top (smallest sizes) and bottom (largest sizes).

Ions	**OA (µL)**	**Longest axis (nm)**	**AR**
100 µL 0.5 M HCl	0	26 ± 6	2.9 ± 0.8
	20	42 ± 7	3.0 ± 0.9
	200	279 ± 89	1.1 ± 0.1
	200	13 ± 3	2.0 ± 0.6
50 µL 0.5 M HCl	0	29 ± 6	3.3 ± 0.9
	20	38 ± 9	3.0 ± 1.1
	200	281 ± 156	1.2 ± 0.2
	200	18 ± 3	2.7 ± 0.6
50 µL 0.25 M NaOH	0	38 ± 7	3.9 ± 1.0
	20	38 ± 7	2.9 ± 0.8
	200	N/A*	N/A*
	200	14 ± 3	2.0 ± 0.8
100 µL 0.25 M NaOH	0	39 ± 5	3.6 ± 0.7
	20	34 ± 7	2.5 ± 0.8
	200	460 ± 171	1.2 ± 0.2
	200	26 ± 37†	2.3 ± 0.6

*Yielded large variety of particle sizes.

†A few large THH were present in the images. If neglected, the length and AR would be 16 ± 3 nm and 2.4 ± 0.6 respectively.

Images for 0 µL OA in Figure 33(a,d,g,j) all display rods. At 20 µL OA there are etched rods for all amounts of ions (b,e,h,k). The bottom products of 200 µL OA (c,f,i,l) gave a variety of large shapes, typically a lot of THH, while the top products displayed mostly tiny rods (Figure 34a-d), with an occasional large THH (see 100 µL 0.25 M NaOH, 200 µL OA).

Figure 35 displays some of the shapes obtained when the ions were added at the start of the synthesis. The samples which had the largest shifts between the differing times of ion-addition in the UV-spectra were selected. All the samples with 100 µL 0.5 M HCl were imaged (35a-d). In addition, all 200 µL OA samples were imaged, and images from 100 µL 0.25 M NaOH are shown in Figure 35e,f.

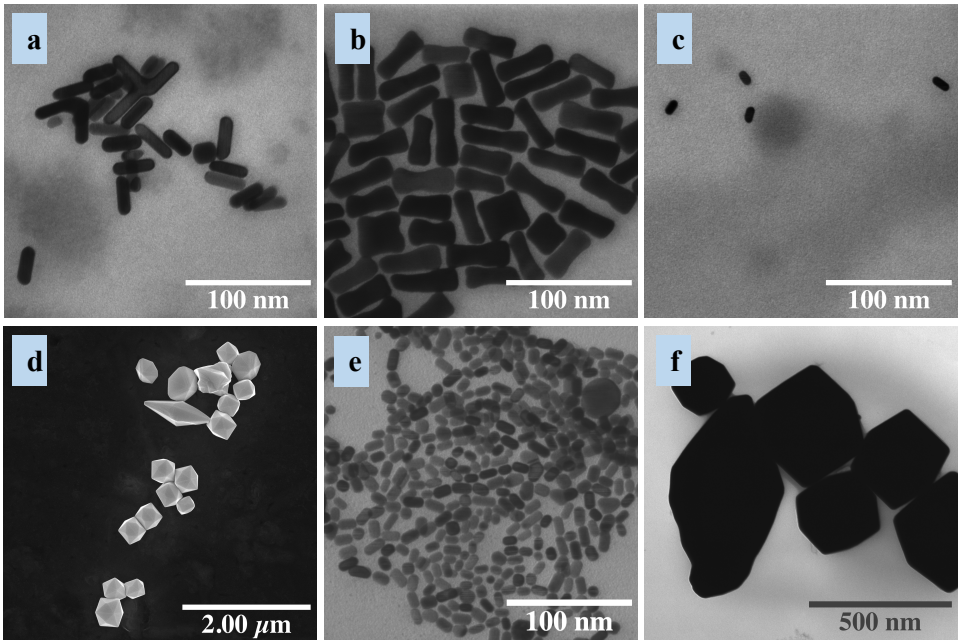

Figure 35: S(T)EM images from ions study (ions added at start). 100 µL 0.5 M HCl; a) 0 µL OA, b) 20 µL OA, c,d) 200 µL OA (top, bottom). 100 µL 0.25 M NaOH; e,f) 200 µL OA (top, bottom).

Average lengths and ARs for ions added at the start are listed in Table 15.

Table 15: Length and AR for AuNPs when ions were added at start. 200 µL has 2 products: top (smallest sizes) and bottom (largest sizes).

Ions	OA (µL)	Longest axis (nm)	AR
	0	28 ± 6	2.9 ± 0.7
100 µL	20	42 ± 8	3.1 ± 1.0
0.5 M HCl	200	337 ± 127	1.2 ± 0.2
	200	13 ± 2	2.0 ± 0.4
50 µL	200	309 ± 133	1.2 ± 0.2
0.5 M HCl	200	15 ± 3	2.3 ± 0.5
50 µL	200	308 ± 198	1.3 ± 0.2
0.25 M NaOH	200	14 ± 2	2.1 ± 0.4
100 µL	200	332 ± 151	1.2 ± 0.2
0.25 M NaOH	200	12 ± 3	1.6 ± 0.3

Comparing the sizes of 0 and 20 µL with 100 µL HCl in tables 14 and 15 reveal that the particles were very similar despite the shift between them in their UV-spectra (Figure 32a). As the remaining particles obtained for 0 and 20 µL OA for other amounts of "ions at start" had even more similar UV-spectra to "ions before AA", these were assumed to be approximately the same and were not imaged. Since the spectra of 200 µL OA (top products) were significantly different for all the variations of ions, they were imaged and measured for all ions.

3.7 Effect of OA and ions

This section discusses the observations made when taking a closer look at the ions and their role in the AuNP synthesis.

When adding the same amount of ions to the system at the start as directly before the addition of AA, there is a difference in pH at the point of adding the reducing agent. From an earlier project [2], it was observed that the solution tended to level out at ∼pH 3 before addition of reducing agent if it was above this value at the start of the synthesis. If it was below pH 3, it would increase only slightly before adding AA. The pH could be thought to have an effect on the reduction potential, but to distinguish between this and the ions effect, it was of essence to check what would happen when the same amount of ions was added at different steps.

The time of the ions being added did not seem to have a major impact on the final NPs despite the differences in pH before the addition of AA. The addition of HCl did not have the anticipated effect of lowering the pH when adding directly before addition of AA, but rather increased it slightly (see 50 µL HCl in Table 13). The amount of HCl added was likely not strong enough to reduce the pH significantly. For all samples with

NaOH, the pH before addition of reducing agent was slightly lower for "ions at start". As the particles gave the same UV for these despite the difference in pH for the time of AA addition, it seems that the amount of ions had a greater impact on the final shapes than the pH they resulted in.

From the UV-Vis spectra in 32 it was evident that the clearest differences were according to the amount of OA in the syntheses. Higher amount of OA (200 µL) leads to some bottom-product in all the experiments. The single broad peak obtained for all these (A.6) could indicate that the samples had a wide variety of shapes and aspect ratios. However, it could also be as a result of the particles being too large and not resulting in the same amount of absorbance as the smaller particles (ref. section 1.1).

Sizes observed for the bottom products of 200 µL OA in "ions before AA" (Figure 35d,f, Table 15) differ somewhat from the corresponding products of "ions at start" (Figure 33c,l, Table 14). However, these are considered to be almost the same for all the samples, as the particles were very large, and the measurements could be heavily affected by the bias from the S(T)EM imaging. Notice that the top product of these samples differed from those in the initial studies (section 3.3). These were smaller, and larger particles (>100 nm) were only observed for 100 µL NaOH. The earlier 200 µL OA samples were visibly pink with some orange in them, while these were all darker purple/blue. They also gave different UV-spectra.

Similar trends to those in section 3.3 are seen in the size and AR when the amount of ions was altered (Figure 33). 0 µL OA gave increasing lengths with increasing concentration of basic ions, but random values for AR. 20 µL OA yielded smaller particles (shorter length and smaller AR) as the pH increased. The sizes of particles with 200 µL OA could also seem to be increasing with increasing pH.

From section 3.3.1 we saw that the growth of AuNPs was very slow when 200 µL OA was present. It was unclear if the growth was done before it was stopped, which could imply that some of the particles may have grown more if not stopped. Therefore, the higher L with higher pH (as observed for bottom product in Table 14) could be because of particles growing slightly faster with a higher concentration of NaOH in the system.

For the experiments performed, it seems that Oleic acid has a stronger effect on the morphology than the ions.

3.8 Yield

Determining the yield of the synthesis may help in understanding the growth of the AuNPs. Weak reducing conditions are used to allow for the slow growth of anisotropic NPs, and 100 % gold reduction does not hold under these conditions [18]. Therefore, quantifying the amount of ionic Au reduced during the reactions is important in understanding the growth. A yield study using MP-AES was conducted to determine how much of the gold ions added in the reaction are actually converted into AuNPs. The method used in this work is described in section 2.3.4, and some assumptions were made:

- All gold ions from $HAuCl_4$ would react in the synthesis to produce AuNPs in case of 100% yield.
- The detected concentration of gold from the stock solution is the actual concentration of ions added in the reaction.
- No loss of metallic AuNPs during washing.
- No ionic gold in final precipitate solution.
- The amount of Au from the seed solution was neglected

Three replicate runs of the same samples were done. One sample without $AgNO_3$, one with $AgNO_3$, and one with $AgNO_3$ and 20 µL OA. 3 runs of $HAuCl_4$ (from 1mM stock solution used in the syntheses) were analysed and the yield was calculated assuming the amount of Au from these gave the actual concentration of the gold added. The results are presented in Figure 36. The values are furthermore listed in Table 16.

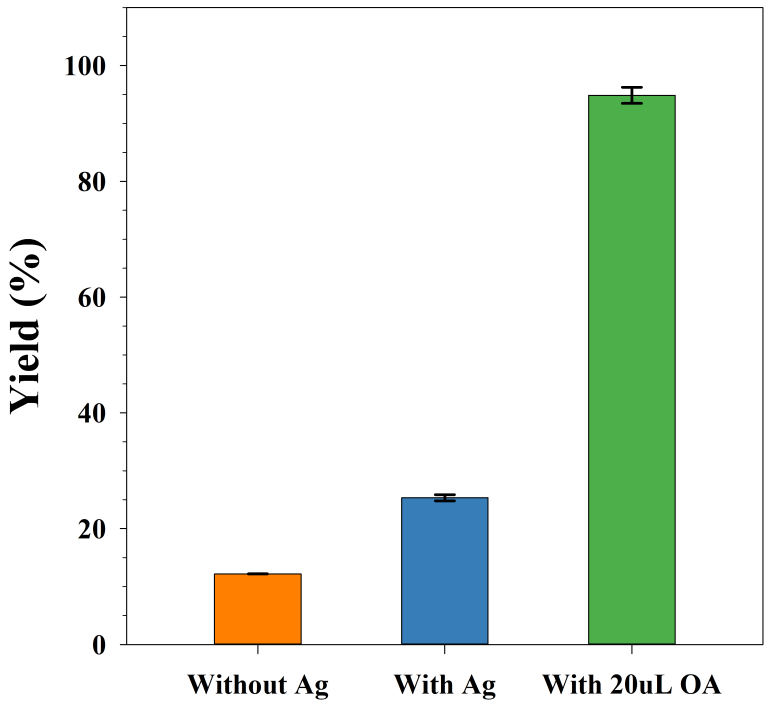

Figure 36: Yield of gold ions in final AuNPs for 3 different syntheses.

Table 16: Yield (%) of 3 different syntheses.

Synthesis	**Yield (%)**
Without $AgNO_3$	12.2 ± 0.0
With $AgNO_3$	25.3 ± 0.5
With $AgNO_3$ & 20 µL OA	94.9 ± 1.4

The yield for AuNRs (synthesis with Ag) obtained in this study was higher than that reported by Orendorff et al.[18]. They reported a yield of ∼14%, detected by Inductively Coupled Plasma Mass Spectrometry (ICP-MS). ICP-MS is a more sensitive technique than MP-AES[41], but the difference may be caused by variations between labs and in the actual synthesis routine.

From this, it is evident that some gold ions present in the growth solution remain unreacted. When 20 µL OA was used in the synthesis, a significantly higher yield was obtained than without. The synthesis without silver gave the lowest yield. This could imply that OA has a strong effect, either in reducing the gold, or in facilitating the growth of AuNPs. This could be a result of the OA acting as a reducing agent which would increase the supersaturation and therefore also the yield.

3.9 Growth mechanism

In this section the growth mechanism of the AuNPs is discussed. This is proposed based on the observations and inferences made for the data that was produced during this work.

The role of pH, ions and OA were the most broadly studied parameters of this work. The most evident differences in morphology were seen when changing from no silver to with silver, to OA amount of 20 and 200 µL (Figure 28). When no silver is present in the solution, mostly spherical or random shapes would form. This supports the claim that the silver has some effect on directing the growth. Typically AuNRs will form when silver is present and no OA is used. This could follow any of the mentioned growth mechanisms (section 1.4).

The role of pH, as discussed in section 3.5, had an effect on the final AuNPs. The most evident effect was seen when the pH was increased to 11 before adding AA, which gave mostly spherical particles independent of the other variations. This could be related to the reduction potential of AA being higher (as mentioned in 1.5.4) and increase in the supersaturation, leading to a rapid growth without much shape control. In case of the silver UPD mechanism (section 1.4), it would make sense as the Ag might not have time to reduce and hinder the growth in the {110}-direction before Au is reduced as well. However, some symmetry-breaking is seen for 20 µL OA, which could point towards the OA participating in creating a stronger micelle soft template than when only CTAB is used. However, since there are mostly spheres, the zipping mechanism might explain why there are a few rods. In this case, some surfactant would have had time to add onto

to the surface as the AuNPs grow, possibly because of a higher concentration of total surfactant concentration. The small spherical particles could also be explained by the heterogeneous nucleation.

For the two amounts of OA studied, two characteristic shapes were typically obtained at all pH values: etched rods for low (20 µL) and THH for high (200 µL) amounts of OA. The products resemble the two shapes as described for overgrowth in section 1.4. However, it may appear that the low amount of OA served mostly as a reducing agent allowing a quicker reduction and facilitating for more rapid growth. This is also supported by the kinetics (section 3.3.1) showing a higher growth rate for syntheses with 20 µL than with $AgNO_3$ without OA. However, it may still have served as a capping agent here but least in the {111} direction, as this is where the etching occurs. This theory could also be supported by the resulting etched rods obtained at high AA amounts, without OA.[1] [20]

When 200 µL OA was present, the micelles might have been more densely packed and thereby slowing the growth significantly. This is slightly counter-intuitive when comparing to the lower amount (20 µL OA) possibly acting more as a reducing agent. However, these large AuNPs (L > 60 nm) could point towards a high reduction, but slow growth because of the amount of surfactant available in the reaction. This could be described in a similar way to the "zipping" mechanism[19], in which more surfactant adds on to the surface as the NPs grow. On the other hand, it could point towards not enough surfactant for the amount of reduced Au, causing the large particles to fall out of the system as bottom product. Also, the stochastic popcorn-mechanism[12] could be supported by the observation that there were separate top-and bottom products. However, this observation could be caused by other factors as well. For instance, the larger products could be growing at the expense of the smaller NPs, providing a more energetically favorable site to grow on.

It should be taken into consideration that assumptions about the growth are made according to what the final product looks like. Additionally, the images obtained from S(T)EM could be biased, and conclusions are drawn from what is captured in the images.

4 Conclusion

The aim of this thesis was to quantify and understand the growth of anisotropic AuNPs further. This was done through an experimental approach and exploring the effects on the final product. The experimental conditions were systematically explored by varying the type (and amount) of reducing agent, the amount of oleic acid, silver, ions (HCl and NaOH) and pH.

Mathematical models were made based on a screening design for TA, OA, $AgNO_3$ and pH. They showed that pH had the most effect on the AR, but there was no clear trend for the lengths. The effective range of $AgNO_3$ (where the AR increased with increasing Ag-amount) for 750 µL 0.1 M TA was determined to be 0.15 - 1.5 mL (4 mM) prior to the design-experiments.

The amount of OA showed a dominating effect on the shape when the pH and amount of ions were varied. When 20 µL OA was used, there was a decreasing size (length and AR) with increasing pH. 200 µL OA gave bottom product for all pH-values, as well as a separate top product.

When changing the pH to 11 directly before adding AA (section 3.4), mostly spheres were seen for synthesis with and without Ag and with 20 µL OA. It was suggested that this was caused by the reduction potential of AA being raised significantly because of it's second pK_a-value. This could also cause a high supersaturation, leading to rapid growth. A higher starting-pH generally led to a quicker growth (section 3.3.1), despite the fact that the pH was approximately the same at the time of adding AA. However, since the growth rate was generally lower than at pH 6 when increased beyond this point, the concentration of ions were considered. The ions were suggested to have a greater effect than the pH (section 3.6), as the time of adding ions had little to no effect on the final product. However, this was only valid up to a certain pH (see pH 11 explained above).

A yield study was conducted using MP-AES for some of the syntheses variations (section 3.8). The yield was found to be 12.2, 25.3 and 94.9 % for syntheses without silver, with silver and with silver and 20 µL OA, respectively. This pointed towards the dual role of OA as co-surfactant and reducing agent.

5 Future work

To further understand the underlying mechanisms and interplay between the factors of the AuNP syntheses, more characterization of particles with varying conditions need to be considered.

To explore the effect of the ions further, the pH could be changed using other acids and bases. Also, continuous pH measurements for tracking the change in pH over time could be of interest to gain further understanding of when reactions occur.

The method described for MP-AES could be used to track how the yield is changing with synthesis parameters. It should however be taken into consideration that a lot of assumptions were made. Some Ag might have been present in the AuNPs, however this was not measured as the amount of this would be significantly lower than the amount of Au, and therefore challenging to detect at these low concentrations. There is room for developing a more robust method/standard procedure for determining the yield using MP-AES. In addition, a method detection limit (MDL) should be determined based on all the steps involved. Ideally the supernatant should also be tested, to make sure this contains the remaining amount of Au assumed to be in the solution.

References

[1] K Raghunathan, J Antony, S Munir, JP Andreassen, S Bandyopadhyay. Tuning and tracking the growth of gold nanoparticles synthesized using binary surfactant mixtures. *Nanoscale Advances*, 2:1980–1992, 2020.

[2] TM Bruns. Tracking Underlying Mechanisms of Anisotropic Gold Nanoparticles. Specialization project, NTNU, 2020.

[3] H Chen, L Shao, Q Li, J Wang. Gold nanorods and their plasmonic properties. *Chemical Society Reviews*, 42:2679–2724, 2013.

[4] SE Lohse, CJ Murphy. The quest for shape control: A history of gold nanorod synthesis. *Chemistry of Materials*, 25:1250–1261, 2013.

[5] CL Nehl, JH Hafner. Shape-dependent plasmon resonances of gold nanoparticles. *Journal of Materials Chemistry*, 18:2415–2419, 2008.

[6] K Sztandera, M Gorzkiewicz, B Klajnert-Maculewicz. Gold Nanoparticles in Cancer Treatment. *Molecular Pharmaceutics*, 16:1–23, 2019.

[7] E Petryayeva, UJ Krull. Localized surface plasmon resonance: Nanostructures, bioassays and biosensing - A review. *Analytica Chimica Acta*, 706:8–24, 2011.

[8] L Meng, J Zhang, H Li, W Zhao, T Zhao. Preparation and Progress in Application of Gold Nanorods. *Journal of Nanomaterials*, 2019, 2019.

[9] M Tréguer-Delapierre, J Majimel, S Mornet, E Duguet, S Ravaine. Synthesis of non-spherical gold nanoparticles. *Gold Bulletin*, 41/2:195–207, 2008.

[10] ND Burrows, S Harvey, FA Idesis, CJ Murphy. Understanding the Seed-Mediated Growth of Gold Nanorods through a Fractional Factorial Design of Experiments. *Langmuir*, 33:1891–1907, 2017.

[11] H-H Chang, MT Gole, CJ Murphy. A golden time for nanotechnology. *MRS Bulletin*, 45:387–393, 2020.

[12] JA Edgar, AM McDonagh, MB Cortie. Formation of gold nanorods by a stochastic "popcorn" mechanism. *ACS Nano*, 6:1116–1125, 2012.

[13] J Polte. Fundamental growth principles of colloidal metal nanoparticles–a new perspective. *CrystEngComm*, 17(36):6809–6830, 2015.

[14] B Ding, Y Li, SY Huang, QQ Chu, CX Li, CJ Li, GJ Yang. Material nucleation/-growth competition tuning towards highly reproducible planar perovskite solar cells with efficiency exceeding 20%. *Journal of Materials Chemistry A*, 5:6840–6848, 2017.

[15] VK LaMer. Nucleation in phase transitions. *Ind Eng Chem*, 44(6):1270–1277, 1952.

[16] W Tong and MJ Walsh and P Mulvaney and J Etheridge and AM Funston. Control of Symmetry Breaking Size and Aspect Ratio in Gold Nanorods: Underlying Role of Silver Nitrate. *The Journal of Physical Chemistry*, 121:3549–3559, 2017.

[17] SK Gundanna, A Mitra, LKG Bhatta, and UM Bhatta. Effect of thermal treatment on the surface/interfacial behaviour of au@ sio2 nanoparticles in the presence of ctab surfactant molecules. *Powder Technology*, 381:503–508, 2021.

[18] CJ Orendorff and CJ Murphy. Quantitation of metal content in the silver-assisted growth of gold nanorods. *The Journal of Physical Chemistry B*, 110(9):3990–3994, 2006.

[19] CJ Murphy, TK Sau, AM Gole, CJ Orendorff, J Gao, L Gou, SE Hunyadi, and T Li. Anisotropic metal nanoparticles: synthesis, assembly, and optical applications. *The Journal of Physical Chemistry B*, 109(29):13857–13870, 2005.

[20] BN Khlebtsov, VA Khanadeev, J Ye, GB Sukhorukov, NG Khlebtsov. Overgrowth of gold nanorods by using a binary surfactant mixture. *Langmuir*, 30:1696–1703, 2014.

[21] B Nikoobakht and MA El-Sayed. Evidence for bilayer assembly of cationic surfactants on the surface of gold nanorods. *Langmuir*, 17(20):6368–6374, 2001.

[22] M Brown, BJ Wiley. Bromide Causes Facet-Selective Atomic Addition in Gold Nanorod Syntheses. *Chemistry of Materials*, 32:6410–6415, 2020.

[23] GG-Rubio, L Scarabelli, AG-Martínez, LM L-Marzán. Surfactant-Assisted Symmetry Breaking in Colloidal Gold Nanocrystal Growth. *ChemNanoMat*, 6:698–707, 2020.

[24] ME Haque, AR Das, AK Rakshit, and SP Moulik. Properties of mixed micelles of binary surfactant combinations. *Langmuir*, 12(17):4084–4089, 1996.

[25] X Ye, C Zheng, J Chen, Y Gao, and CB Murray. Using binary surfactant mixtures to simultaneously improve the dimensional tunability and monodispersity in the seeded growth of gold nanorods. *Nano letters*, 13(2):765–771, 2013.

[26] J Harper-Harris, K Kant, and G Singh. Oleic Acid-Assisted Synthesis of Tunable High-Aspect-Ratio Multiply-Twinned Gold Nanorods for Bioimaging. *ACS Applied Nano Materials*, 4(4):3325–3330, 2021.

[27] S Bandyopadhyay, G Singh, and WR Glomm. Shape tunable synthesis of anisotropic gold nanostructures through binary surfactant mixtures. *Materials Today Chemistry*, 3:1–9, 2017.

[28] B Nikoobakht and MA El-Sayed. Preparation and growth mechanism of gold nanorods (NRs) using seed-mediated growth method. *Chemistry of Materials*, 15(10):1957–1962, 2003.

[29] JK Guillory. The Merck Index: An Encyclopedia of Chemicals, Drugs, and Biologicals Edited by Maryadele J. O'Neil, Patricia E. Heckelman, Cherie B. Koch, and Kristin J. Roman. Merck, John Wiley & Sons, Inc., Hoboken, NJ. 2006. xiv+ 2564 pp. 18× 26 cm. ISBN-13 978-0-911910-001., 2007.

[30] D Roy, Y Xu, R Rajendra, L Wu, P Bai, and N Ballav. Gold Nanoearbuds: seed-

mediated synthesis and the emergence of three plasmonic peaks. *The journal of physical chemistry letters*, 11(9):3211–3217, 2020.

[31] R Rajendra, PK Gangadharan, S Tripathi, S Kurungot, and N Ballav. High-index faceted Au nanocrystals with highly controllable optical properties and electrocatalytic activity. *Nanoscale*, 8(46):19224–19228, 2016.

[32] R Rajendra, D Roy, S Tripathi, and N Ballav. Facile synthesis of concave cuboid Au NCs with precisely tunable dimensions and mechanistic insight. *Langmuir*, 35(29):9456–9463, 2019.

[33] H-Y Wu, M Liu, and MH Huang. Direct synthesis of branched gold nanocrystals and their transformation into spherical nanoparticles. *The Journal of Physical Chemistry B*, 110(39):19291–19294, 2006.

[34] Y Xu, L Chen, X Ye, X Wang, J Yu, Y Zhao, M Cao, Z Xia, B Sun, and Q Zhang. Cooperative interactions among CTA+, Br–and Ag+ during seeded growth of gold nanorods. *Nano research*, 10(6):2146–2155, 2017.

[35] L Roach, S Ye, SCT Moorcroft, K Critchley, PL Coletta, and SD Evans. Morphological control of seedlessly-synthesized gold nanorods using binary surfactants. *Nanotechnology*, 29(13):135601, 2018.

[36] L Vigderman and ER Zubarev. "High-yield synthesis of gold nanorods with longitudinal SPR peak greater than 1200 nm using hydroquinone as a reducing agent". *Chemistry of Materials*, 25(8):1450–1457, 2013.

[37] CJ Murphy, LB Thompson, AM Alkilany, PN Sisco, SP Boulos, ST Sivapalan, JA Yang, DJ Chernak, J Huang. The many faces of gold nanorods. *Journal of Physical Chemistry Letters*, 1:2867–2875, 2010.

[38] W Mäntele and E Deniz. *UV–VIS absorption spectroscopy: Lambert-Beer reloaded*. Elsevier, 2017.

[39] S Bandyopadhyay. *Fabrication and Applications of Nanomaterials*. McGraw-Hill, 1st edition, 2019.

[40] Agilent Technologies. *Microwave Plasma Atomic Emission Spectroscopy (MP-AES)*. Jan. 2021 edition, 2016. Application eHandbook. Accessed: 2021-07-27.

[41] V Balaram. Microwave plasma atomic emission spectrometry (MP-AES) and its applications–A critical review. *Microchemical Journal*, page 105483, 2020.

[42] B Vysetti, D Vummiti, P Roy, C Taylor, CT Kamala, M Satyanarayanan, P Kar, KSV Subramanyam, AK Raju, and K Abburi. Analysis of geochemical samples by microwave plasma-AES. *Atomic Spectroscopy*, 35(2):65–78, 2014.

[43] S Borse, S Joshi, and A Khan. Enhanced in vitro cytotoxicity and cellular uptake of DNA bases functionalized gold nanoparticles in HeLa cell lines. *RSC advances*, 5(18):13402–13410, 2015.

[44] K Zürbes. Status update, Kick-off Meeting Nano-Syn-Sens. Powerpoint presentation, NTNU, 2020.

A Appendix

A.1 Abbreviations

A list of abbreviations used throughout the report is provided in this section.

AA	=	Ascorbic Acid
AR	=	Aspect ratio (Length/Diameter)
AuNPs	=	Gold nanoparticles
AuNRs	=	Gold nanorods
CTAB	=	Hexadecyltrimethylammonium bromide
DOE	=	Design of Experiments
LSPR	=	Localized Surface Plasmon Resonance
MP-AES	=	Microwave Plasma Atomic Emission Spectrometry
NaOL	=	Sodium Oleate
NPs	=	Nanoparticles
OA	=	Oleic Acid
S(T)EM	=	Scanning (Transmission) Electron Microscopy
TA	=	Tannic Acid
TEM	=	Transmission Electron Microscopy
THH	=	Tetrahexahedra
UPD	=	Under-Potential Deposition

A.2 List of all experiments

A list of all the details of each synthesis variation is given in Table A1. The varied parameters of interest are given in orange.

Table A1: All synthesis variations

Category	Details	Starting-pH varied	pH befoe AA varied	0.5 M HCl (uL)	0.25 M NaOH (uL)	OA (uL)	AgNO3 (uL)	AA (uL)	TA (uL)
TA	150 uL Ag			0	0	0	150	0	750
TA	720 uL Ag			0	0	0	720	0	750
TA	1290 uL Ag			0	0	0	1290	0	750
TA	1860 uL Ag			0	0	0	1860	0	750
TA	2430 uL Ag			0	0	0	2430	0	750
TA	3000 uL Ag			0	0	0	3000	0	750
TA_DOE	1		11			0	825	0	100
TA_DOE	2		1.5			100	150	0	100
TA_DOE	3		6.25			0	150	0	100
TA_DOE	4		11			0	1500	0	1650
TA_DOE	5		6.25			100	1500	0	1650
TA_DOE	6		1.5			100	825	0	1650
TA_DOE	7		6.25			50	825	0	875
TA_DOE	8		11			100	150	0	875
TA_DOE	9		11			100	1500	0	100
TA_DOE	10		1.5			0	150	0	1650
TA_DOE	11		1.5			0	1500	0	875
TA_DOE	12		1.5			50	1500	0	100
TA_DOE	13		11			50	150	0	1650
pH @ start	no Ag	11				0	0	135	0
pH @ start	Ag	11				0	750	135	0
pH @ start	20 uL OA	11				20	750	135	0
pH @ start	200 uL OA	1.5				200	750	135	0
pH @ start	200 uL OA	3				200	750	135	0
pH @ start	200 uL OA					200	750	135	0
pH @ start	200 uL OA	10				200	750	135	0
pH bf AA	no Ag		11			0	0	135	0
pH bf AA	Ag		11			0	750	135	0
pH bf AA	20 uL OA		11			20	750	135	0
ions @ start				100	0	0	750	135	0
ions @ start				50	0	0	750	135	0
ions @ start				0	50	0	750	135	0
ions @ start				0	100	0	750	135	0
ions @ start				100	0	20	750	135	0
ions @ start				50	0	20	750	135	0
ions @ start				0	50	20	750	135	0
ions @ start				0	100	20	750	135	0
ions @ start				100	0	200	750	135	0
ions @ start				50	0	200	750	135	0
ions @ start				0	50	200	750	135	0
ions @ start				0	100	200	750	135	0
ions bf AA				100	0	0	750	135	0
ions bf AA				50	0	0	750	135	0
ions bf AA				0	50	0	750	135	0
ions bf AA				0	100	0	750	135	0
ions bf AA				100	0	20	750	135	0
ions bf AA				50	0	20	750	135	0
ions bf AA				0	50	20	750	135	0
ions bf AA				0	100	20	750	135	0
ions bf AA				100	0	200	750	135	0
ions bf AA				50	0	200	750	135	0
ions bf AA				0	50	200	750	135	0
ions bf AA				0	100	200	750	135	0

A.3 Supernatant

Figure A1 shows the colour of supernatant after washing when particles are still in the supernatant (red at top). These samples are from adjusting to pH 11 before adding AA. To the left: with $AgNO_3$, to the right: without $AgNO_3$.

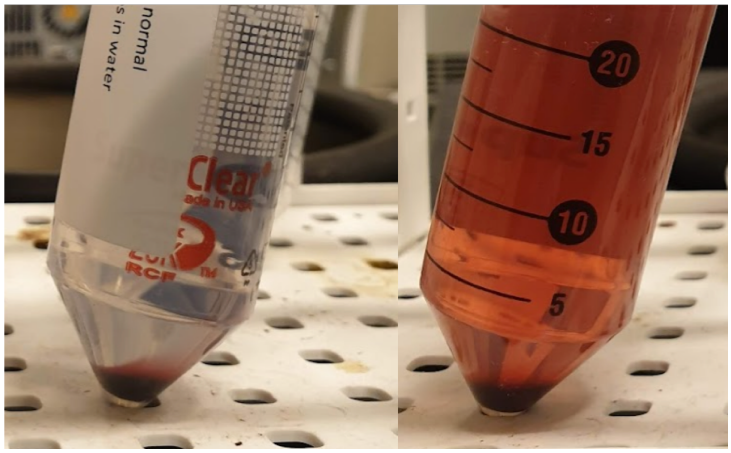

Figure A1: Precipitate (at bottom) and supernatant while washing AuNPs.

A.4 Area under the curve

The following MATLAB code was used to calculate the area under the curve for the kinetics experiments.

```
clc
num = xlsread('data.xls'); %input data file name
x = num (:,1);
d = size (num);
int= 0;
for n= 2:d(1,2)

int(n-1) = trapz (x,num(:,n));
end
int = int';
filename = data.xls'; %input data file name
xlswrite(filename, int, 'Area', 'A'); %input new file name
disp(int);
```

A.5 S(T)EM of 200µL OA Bottom Products

During the experiments with a high amount of OA (200µL) (in section 3.3) the samples gave similar products for all pH values. Figure A2 displays representative images of all these products.

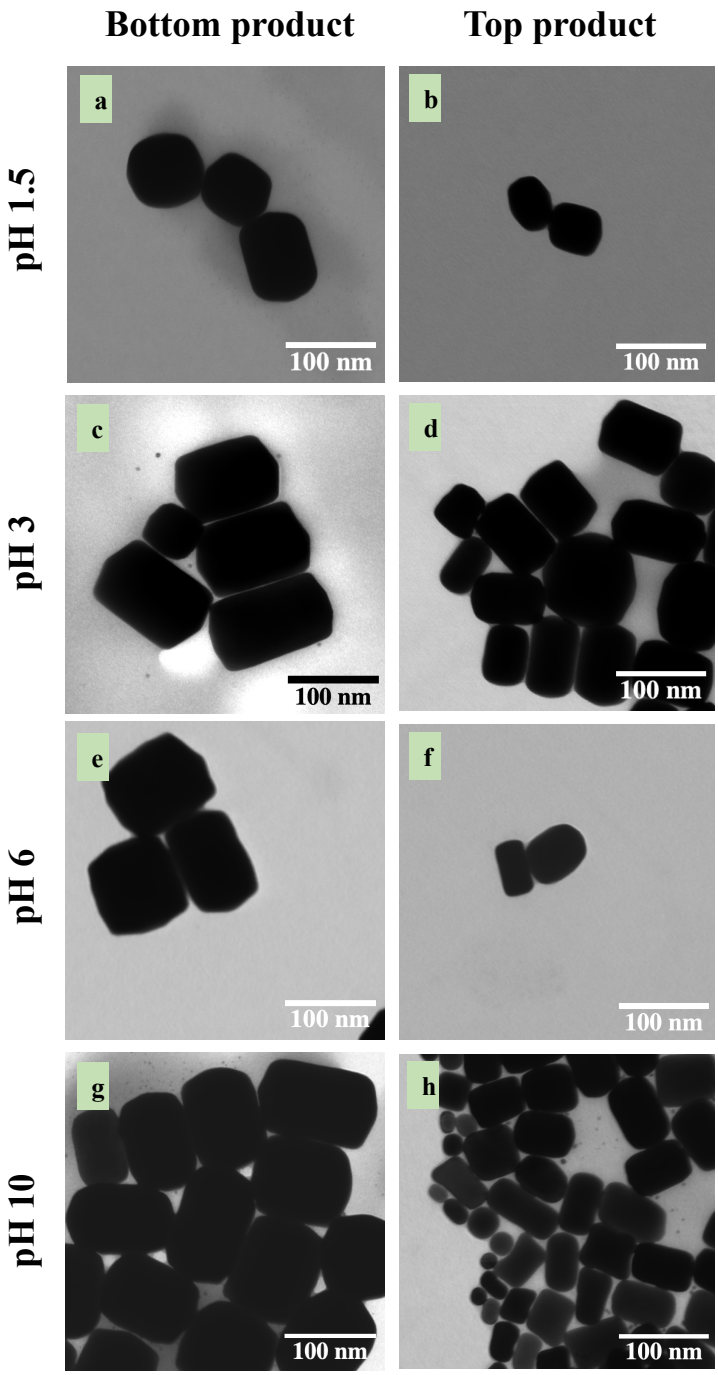

Figure A2: S(T)EM images from varying starting pH with 200µL OA.

A.6 UV-Vis of ions-study Bottom Product

When studying AuNPs grown with 200 µL OA (see section 3.6), the bottom product typically gave similar results. UV-spectra of these from the ions study are displayed in Figure A3.

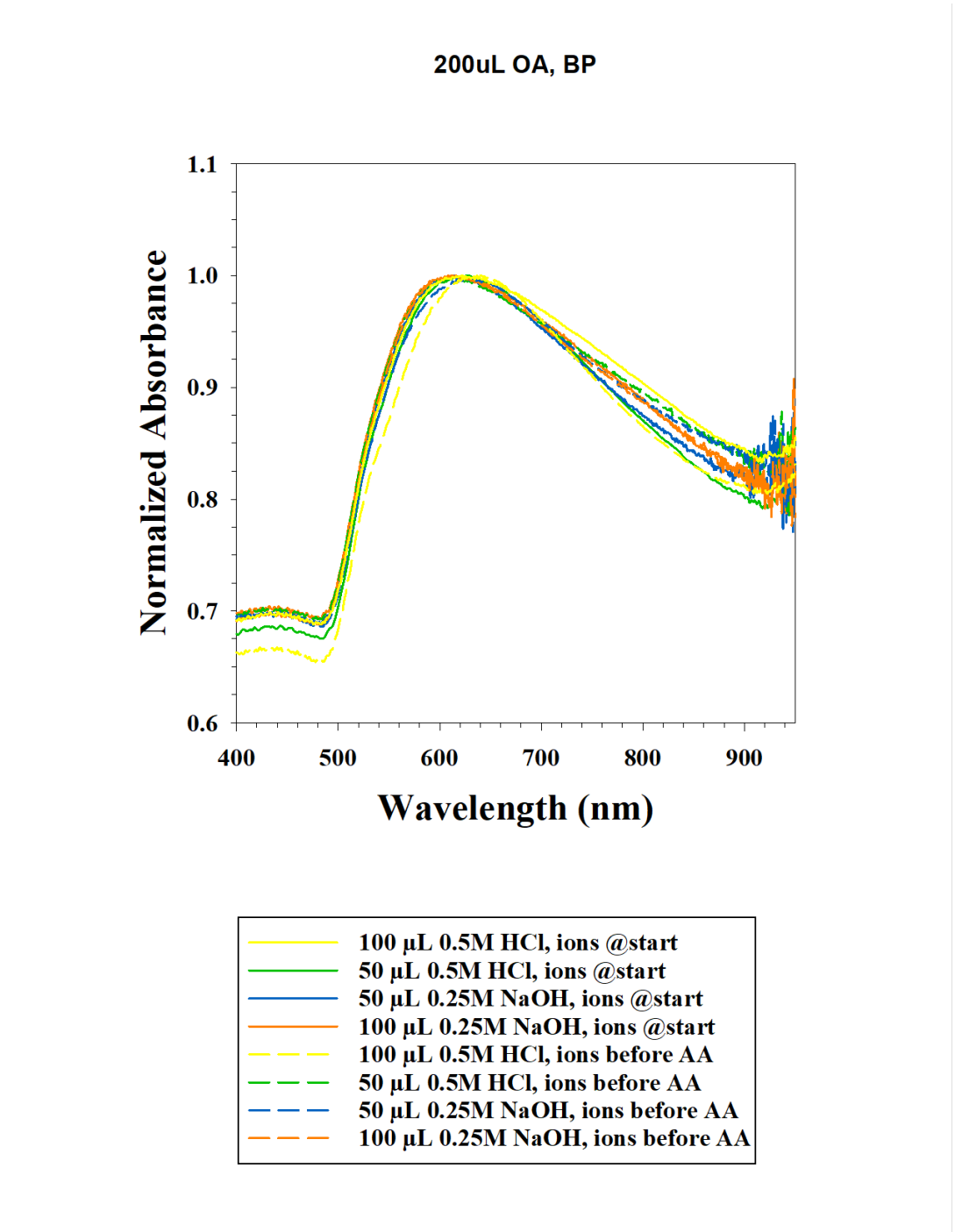

Figure A3: UV-Vis of bottom product obtained when studying the effect of ions.

A.7 Notes on synthesis

When synthesizing AuNPs, things may not always go according to plan. Knowing helpful tricks and noticing subtle details along the way may help in getting the synthesis right and identifying if something has gone wrong. This section provides an informal list of things observed during this work that may help others along the way in their experiments.

- The seed-solution should have a clear brown colour and some sparkles may appear towards usage time. If it gets cloudy/shiny after 30 min, it may be because of CTAB crystallizing out. Should be kept at about 25°C to avoid this.
- When conducting experiments with 200 µL OA: heat only until dissolved, and cool on another (colder) heater to avoid evaporation. The solution can become very viscous if heated for too long.
- If the growth solution does not change colour after adding the seed and the solution is not completely blank (has a hint of yellow), then the Au^{3+} (yellow in colour) may not have completely reduced to Au^{1+} (clear). Synthesis failed and needs to be redone. Next time, make sure to wait longer before adding seed. However, be aware that some reactions are very slow and may take longer before colouring the solution.
- Slow-growing AuNP solutions should be stopped at the same time when compared. The growth solution may get darker with time, as water could evaporate while the particles are left to grow at 35°C.

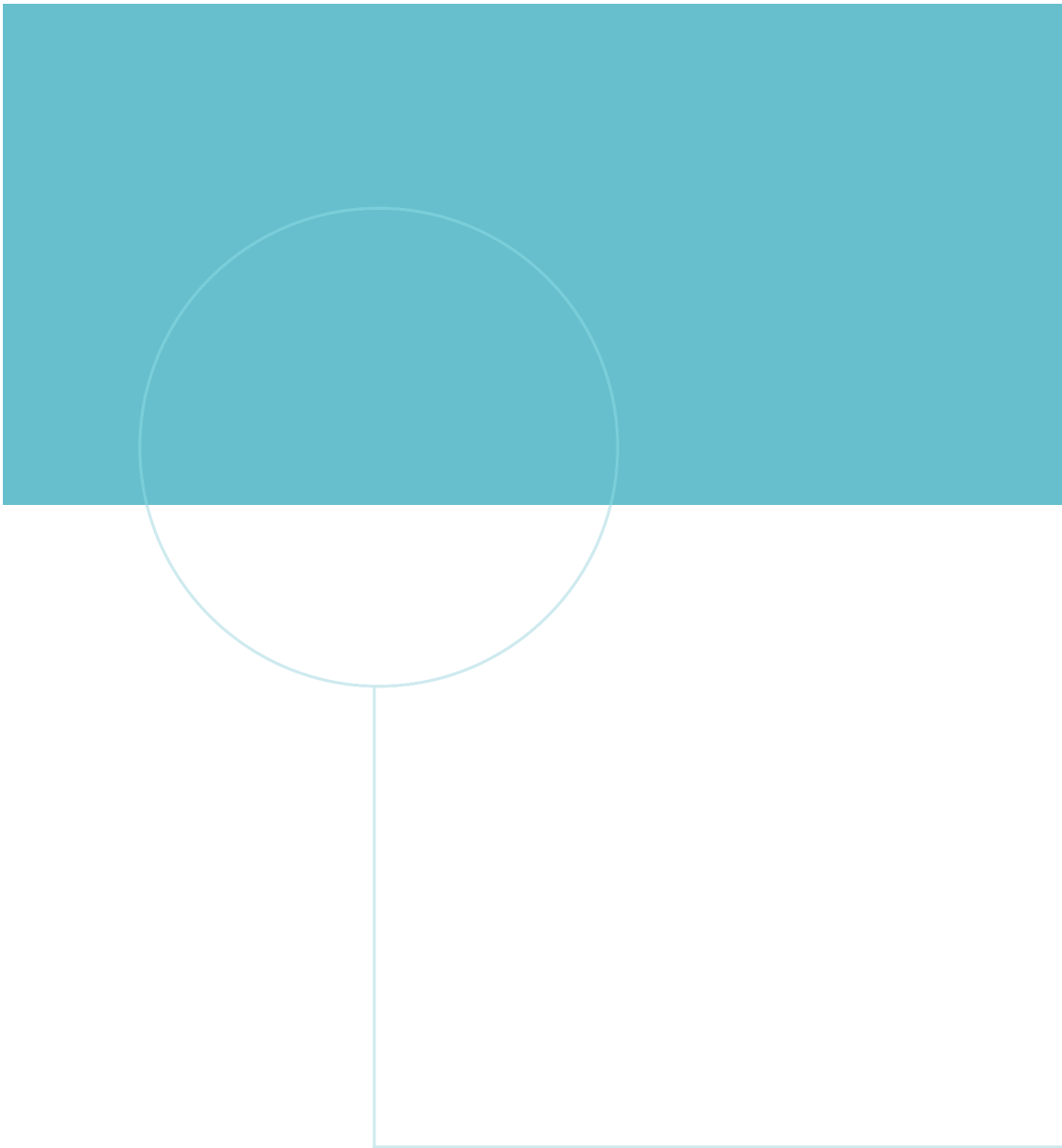

NTNU

Norwegian University of
Science and Technology